NASA TECHNICAL NOTE

NASA TN D-7097

NASA TN D-7097

NUMERICAL METHOD FOR DESIGN OF MINIMUM-DRAG SUPERSONIC WING CAMBER WITH CONSTRAINTS ON PITCHING MOMENT AND SURFACE DEFORMATION

by Russell B. Sorrells and David S. Miller

Langley Research Center
Hampton, Va. 23365

NATIONAL AERONAUTICS AND SPACE ADMINISTRATION • WASHINGTON, D. C. • DECEMBER 1972

1. Report No.	2. Government Accession No.	3. Recipient's Catalog No.
NASA TN D-7097		

4. Title and Subtitle	5. Report Date
NUMERICAL METHOD FOR DESIGN OF MINIMUM-DRAG SUPERSONIC WING CAMBER WITH CONSTRAINTS ON PITCHING MOMENT AND SURFACE DEFORMATION	December 1972
	6. Performing Organization Code

7. Author(s)	8. Performing Organization Report No.
Russell B. Sorrells and David S. Miller	L-8585
	10. Work Unit No.
9. Performing Organization Name and Address	501-06-01-04
NASA Langley Research Center Hampton, Va. 23365	11. Contract or Grant No.
	13. Type of Report and Period Covered
12. Sponsoring Agency Name and Address	Technical Note
National Aeronautics and Space Administration Washington, D.C. 20546	14. Sponsoring Agency Code

15. Supplementary Notes

16. Abstract

This report presents a numerical method, based on linearized theory, for designing minimum-drag supersonic wing camber surfaces of arbitrary planform for a given lift, with options for constraining the pitching moment and/or the surface deformation at the trailing edge of the root chord and for selecting any desired combination of eight specified wing-loading distributions to be employed in the optimization procedure. Two examples are presented to illustrate applications of the method. The results indicate that relatively small drag penalties are incurred in designing wings to be self-trimming and to have a reasonable camber surface.

17. Key Words (Suggested by Author(s))	18. Distribution Statement
Supersonic, Wings, Camber, Design, Minimum drag, Wing camber, Pitching moment, Constraints	Unclassified – Unlimited

19. Security Classif. (of this report)	20. Security Classif. (of this page)	21. No. of Pages	22. Price*
Unclassified	Unclassified	47	$3.00

*For sale by the National Technical Information Service, Springfield, Virginia 22151

NUMERICAL METHOD FOR DESIGN OF MINIMUM-DRAG SUPERSONIC WING CAMBER WITH CONSTRAINTS ON PITCHING MOMENT AND SURFACE DEFORMATION

By Russell B. Sorrells and David S. Miller
Langley Research Center

SUMMARY

This report presents a numerical method, based on linearized theory, for designing minimum-drag supersonic wing camber surfaces of arbitrary planform for a given lift, with options for constraining the pitching moment and/or the surface deformation at the trailing edge of the root chord and for selecting any desired combination of eight specified wing-loading distributions to be employed in the optimization procedure. Two examples are presented to illustrate applications of the method. The results indicate that relatively small drag penalties are incurred in designing wings to be self-trimming and to have a reasonable camber surface.

INTRODUCTION

The performance benefits of twist and camber when applied to swept wings with subsonic leading edges have been demonstrated both theoretically (refs. 1 to 4) and experimentally (refs. 5 to 7). Frequently, however, the theoretical solution for optimum twist and camber results in impractical camber-surface slopes near the wing root. Furthermore, the resulting wing may or may not be self-trimming at the design lift coefficient.

The wing-design procedure presented in this report is a logical extension of the numerical method based on linear theory described in reference 3 and is intended to provide a more versatile system for the design of supersonic wings. Whereas the method as applied in reference 3 determines a combination of three specified wing-loading distributions that produces minimum drag for a given lift, the present design system provides the user the option of selecting any combination of eight specified wing-loading distributions for minimizing drag with a given lift, zero pitching moment about a given reference point, and a given ordinate at the trailing edge of the root chord.

To illustrate the application of the present method and to give some indication of benefits to be gained, two examples are presented.

SYMBOLS

$A(L,N)$ weighting factor applied to leading-edge grid element (see eq. (3))

A_i load strength factor for ith loading

b wing span

c local chord

$\bar{c}$ mean geometric chord

C_D drag coefficient

$C_{D,ij}$ drag coefficient of interference between ith and jth specified loadings (see eq. (20) of ref. 3)

C_L lift coefficient

$C_{L,des}$ design lift coefficient

C_m pitching-moment coefficient, $\frac{\text{Pitching moment}}{qS\bar{c}}$

ΔC_p lifting pressure coefficient

$$F = \sum_{k=1}^{k=a} \lambda_k \varphi_k + C_D = \sum_{k=1}^{k=a} \lambda_k \varphi_k + \frac{1}{2} \sum_{i=1}^{i=n} \sum_{j=1}^{j=n} A_i A_j C_{D,ij}$$

L,N designation of influencing grid elements (see fig. 3)

L^*,N^* designation of receiving grid elements (see fig. 3)

l length of wing root chord

M Mach number

q free-stream dynamic pressure

$\overline{R}$ average value of influence function within a grid element (see eq. (2))

S	reference wing area
x,y,z	Cartesian coordinates (see fig. 2)
x'	distance from wing leading edge measured in x-direction
$z_c(x,y)$	camber-surface z-ordinate at x,y
z_r	camber-surface z-ordinate at wing-root trailing edge
$\beta = \sqrt{M^2 - 1}$	
λ_L	Lagrange multiplier for lift constraint
λ_m	Lagrange multiplier for moment constraint
λ_z	Lagrange multiplier for z_r constraint
φ_k	constraining relation

Subscripts:

1,2,3,...,8	specified loadings
a	number of constraints
i,j	ith and jth specified loadings
k	kth constraint relation
le	leading edge
max	maximum
min	minimum
n	number of specified loadings

NUMERICAL DESIGN METHOD

Objectives

The primary objectives of the present design method are: (1) To achieve low trim drag through use of a pitching-moment constraint, (2) to provide for more versatility in determining an optimum camber surface by increasing the number of specified loadings, and (3) to insure practical camber surfaces by imposing a surface-deformation constraint. When insufficient pitching moment is generated by the unconstrained design procedure (see fig. 1), additional pitching moment must be acquired by deflecting control surfaces. When the control surfaces are close coupled, like those shown in figure 1, substantial increases in trimmed drag sometimes result. An alternate approach is to include a pitching-moment constraint in the wing twist and camber design procedure. This additional constraint will result in a drag at the design C_L (see dashed line in fig. 1) which in most cases will be less than that resulting from trimming by control-surface deflection.

General Procedure

In general, linearized theory is applied to a wing of arbitrary planform and zero thickness lying in the xy-plane, and the camber surface is calculated for each of the eight specified loadings (to be discussed in detail later). The wing lift and pitching-moment coefficients for each of the eight specified loadings, and the wing interference-drag coefficients between any two loadings, are calculated. Lagrange's method of undetermined multipliers is used to minimize drag by determining for each of the eight loadings the weighting factor that satisfies the constraints of a given lift, zero pitching moment, and a given z_C ordinate at the wing-root trailing edge.

Camber Surface and Force Data for a Specified Loading

The wing design procedure presented in this report is an extension of the numerical method described in reference 3. The numerical method of determining the camber surface and force data for a specified loading is identical with that of reference 3, and a less detailed discussion of the theory and the numerical method used is presented here.

Figure 2 illustrates a typical wing planform described by a rectangular Cartesian coordinate system. Linearized theory for supersonic flow is employed to define the camber surface required to support a specified pressure-loading distribution. Numerical implementation of the theory utilizes the concept of Mach boxes, in which a grid system (see fig. 3) is superimposed on the Cartesian coordinate system. (Fig. 3 is illustrative only; in application many more grid elements would be employed.) The symbols L and N denote the position of a particular influencing grid element; L^* and N^* denote the position of the element receiving the influence. The region of integration, originally

bounded by the wing leading edge and the forward Mach lines from L^*,N^*, now consists of a set of grid elements approximating that region, as shown by the shaded area in figure 3. The wing surface slope at a point represented by L^* and N^* may now be found by summing contributions of all elements within the influencing region by the expression (eq. (10) of ref. 3):

$$\frac{\partial z_c}{\partial x}(L^*,N^*) = -\frac{\beta}{4}\Delta C_p(L^*,N^*) + \frac{\beta}{4\pi}\sum_{N=N_{min}}^{N=N_{max}}\sum_{L=1+\lfloor x_{le}\rfloor}^{L=L^*-|N^*-N|}\bar{R}(L^*-L,N^*-N)A(L,N)\Delta C_p(L,N) \tag{1}$$

where the brackets in $\lfloor x_{le}\rfloor$ designate the whole-number part of the quantity. The function $\bar{R}$ may be thought of as the average value of an influence function within a grid element at L,N relating the local loading at element L,N to its influence in determining the necessary slope at downstream element L^*,N^*. This function $\bar{R}$ is given by the expression (eq. (8) of ref. 3):

$$\bar{R}(L^*-L,N^*-N) = \frac{\sqrt{(L^*-L+0.5)^2-(N^*-N-0.5)^2}}{(L^*-L+0.5)(N^*-N-0.5)}$$

$$-\frac{\sqrt{(L^*-L+0.5)^2-(N^*-N+0.5)^2}}{(L^*-L+0.5)(N^*-N+0.5)} \tag{2}$$

A graphical representation of this factor is shown in figure 4. Note the small variations of the factor in the x- or L-direction in contrast to the drastic variations in the Y- or N-direction.

The term $A(L,N)$ in equation (1) is a weighting factor which eliminates the necessity of accepting or rejecting complete block elements and thus permits a better definition of the wing leading-edge shape, which has been found to be extremely critical. The factor $A(L,N)$ takes on values from 0 to 1 given by

$$\left.\begin{aligned} A(L,N) &= 0 && (L - x_{le} \leqq 0)\\ A(L,N) &= L - x_{le} && (0 < L - x_{le} < 1)\\ A(L,N) &= 1 && (L - x_{le} \geqq 1) \end{aligned}\right\} \tag{3}$$

The section lift and pitching-moment coefficients for each of the eight specified loadings and the section interference-drag coefficients between any two loadings i,j are then calculated. The wing lift coefficient $C_{L,i}$ and pitching-moment coefficient $C_{m,i}$ for each of the eight specified loadings and the wing interference-drag coefficients $C_{D,ij}$

between any two loadings i,j are calculated by spanwise summations of the section data. (See eqs. (16), (17), (18), and (20) of ref. 3.)

The Eight Specified Wing-Loading Distributions

The wing design method described in reference 3 employs the following three specified wing-loading distributions: uniform, linear chordwise, and linear spanwise. In the present method, five additional wing-loading distributions are provided so the drag minimization procedure will have more versatility in computing the optimum combination of loadings. This is particularly important in the present method because of the more stringent requirement of satisfying three constraints rather than just one. The eight specified wing-loading distributions presently available are illustrated in figure 5 for a delta wing, and the advantages and disadvantages of applying these loading distributions are discussed in the two illustrative examples.

Optimum Combination of Loadings

In reference 3 Lagrange's method of undetermined multipliers has been applied to the problem of selecting the combination of three loadings that yields a minimum drag for a given lift. In the present report this technique is again employed to minimize drag by selecting the combination of eight loadings which satisfies constraints placed on lift, pitching moment, and z-ordinate at the wing-root trailing edge.

The total pitching-moment coefficient resulting from n wing-loading distributions is given by

$$C_m = \sum_{i=1}^{i=n} C_{m,i} A_i \tag{4}$$

where $C_{m,i}$ denotes the pitching-moment coefficient of the ith loading and A_i is the load strength factor for the ith loading. Similarly, the z-ordinate at the wing-root trailing edge resulting from n wing-loading distributions is given by

$$z_r = \sum_{i=1}^{i=n} z_{r,i} A_i \tag{5}$$

where $z_{r,i}$ denotes the z-ordinate at the wing-root trailing edge on the camber surface required to support the ith loading.

If, in addition to a given lift, the constraints of zero pitching moment $(C_m = 0)$ and given z_r are imposed on the drag-minimization problem, the method of Lagrange multi-

pliers yields the following set of equations which establishes the relative strength of each loading (see ref. 8):

$$\left.\begin{aligned}
&\lambda_L C_{L,1} + \lambda_m C_{m,1} + \lambda_z z_{r,1} + \sum_{i=1}^{i=n} C_{D,1i} A_i = 0 \\
&\lambda_L C_{L,2} + \lambda_m C_{m,2} + \lambda_z z_{r,2} + \sum_{i=1}^{i=n} C_{D,2i} A_i = 0 \\
&\quad\vdots \\
&\lambda_L C_{L,n} + \lambda_m C_{m,n} + \lambda_z z_{r,n} + \sum_{i=1}^{i=n} C_{D,ni} A_i = 0 \\
&\sum_{i=1}^{i=n} C_{L,i} A_i - C_{L,des} = 0 \\
&\sum_{i=1}^{i=n} C_{m,i} A_i = 0 \\
&\sum_{i=1}^{i=n} z_{r,i} A_i - z_r = 0
\end{aligned}\right\} \qquad (6)$$

The first n equations of equations (6) are of the form $\frac{\partial F}{\partial A_i} = 0$ where $F = \sum_{k=1}^{k=a} \lambda_k \varphi_k + C_D$. The expressions $\varphi_k = 0$ are the constraining relations for lift, pitching moment, and z-ordinate at the wing-root trailing edge. These constraining relations form the last three equations of equations (6). The load strength factors A_i, which determine the relative strength of each loading for minimum drag, are solved for, and the camber surface for the minimum-drag combination is determined from

$$z_c(x,y) = \sum_{i=1}^{i=n} z_{c,i}(x,y) A_i \qquad (7)$$

Program Description

The numerical design method has been programed for the CDC 6600 computer. See appendix A for a description of the input required and appendix B for a description of the output. This program requires a storage of 55K octal.

Several options are provided for the user. Any or all of the eight specified loadings shown in figure 5 can be used; also, the pitching-moment constraint ($C_m = 0$) and/or the z constraint (specified value of z_r) can be requested along with the lift constraint (specified $C_{L,des}$) in the computer program input (see appendix A).

ILLUSTRATIVE EXAMPLES

Wing Planforms

To illustrate and establish the validity of the numerical method, a series of example cases is presented for two wing planforms. The results for planform A are presented in figures 6 to 11, and the results for planform B are presented in figures 12 to 17. Wing planform A is representative of a high Mach cruise vehicle, and for the purpose of demonstration the wing design procedure is applied at $M = 3.5$; wing planform B is representative of a highly maneuverable low-supersonic aircraft, and the wing design procedure is applied at $M = 1.4$.

Planform A

Example cases.- Each application presented for wing planform A is denoted by a case number, as described in the following table:

Case	Description
1	Eight loadings, 11 spanwise stations, design for given lift with C_m constraint
2	Eight loadings, 27 spanwise stations, design for given lift with C_m constraint
3	Eight loadings, 51 spanwise stations, design for given lift with C_m constraint
4	Eight loadings, 27 spanwise stations, design for given lift with C_m and z_r constraints
5	Three loadings, 27 spanwise stations, design for given lift with C_m and z_r constraints
6	Case 3 with modified camber at $\frac{y}{b/2} = 0$
7	Eight loadings, 27 spanwise stations, no C_m or z_r constraints

Moment reference location.- Wing planform A is shown in figure 6 with the moment reference location which was selected for all seven cases. This moment reference location represents the center of gravity that will provide for a subsonic static margin of $0.05\bar{c}$ as calculated by the Langley subsonic aerodynamic program A2794 (see ref. 9).

Program A2794 has given good correlation with experimental static-margin data (see ref. 10) and should be a valuable design tool in conjunction with supersonic camber design with moment constraint.

Effect of number of spanwise computation stations.- It was found that the number of spanwise computation stations (see JBYMAX in appendix A) significantly affects the solution. This is believed to be due to the numerical technique currently used in the program to integrate the section lift, drag, and pitching-moment coefficients to obtain the wing lift, drag interference, and pitching-moment coefficients $(C_{L,i},\ C_{D,ij},\ C_{m,i})$.

Figure 7 illustrates the effect of the number of spanwise computation stations on some representative lifting pressure distributions and camber surfaces from the design program, and the longitudinal aerodynamic characteristics from the evaluation program (see ref. 11). The evaluation program was used to substantiate the results of the design program for a $C_{L,des}$ of 0.10. (Preliminary experimental data indicate that a $C_{L,des}$ of 0.10 is too high for Mach 3.5 and that theoretically predicted pressures will not be realized.) The evaluation program also complements the design program in that it provides the drag and pitching-moment characteristics throughout the lift-coefficient range for a given camber surface. Figure 7(c) indicates that the moment constraint produced zero pitching-moment coefficient at $C_{L,des}$ for each case shown, and the drag decreased slightly with increased number of spanwise computation stations.

Although the parameters have been nondimensionalized, the camber lines at the top of figures 7(b), 9(b), and 10(a) $\left(\text{variation of } \frac{z_c}{lC_{L,des}} \text{ with } x/l\right)$ are plotted to such a scale that the slopes represent the true camber slopes for $C_{L,des} = 0.10$. The camber-line slopes for 11 spanwise computation stations are not as severe as those for 27 and 51 stations, but the results shown in figure 8 indicate that at least 27 stations should be used. Figure 8 shows the variation of drag-due-to-lift factor with number of spanwise computation stations. Results from the design program show no significant variation in drag-due-to-lift factor between 27 and 51 spanwise computation stations. Also, the agreement between the design and evaluation programs is better for 27 and 51 stations than for 11 stations. It is believed that the differences between the two programs are accounted for by the fact that the evaluation program must extract lifting-element slopes in the streamwise direction from the camber-surface y,z ordinates which were provided by the design program. These slopes are not necessarily in exact agreement with those used in the design program.

Use of z_r constraint and effect of number of loadings used.- Since the camber surfaces shown in figure 7(b) for cases 2 and 3 drop excessively at the root chord, a z_r constraint value of $-1.27lC_{L,des}$ was added for cases 4 and 5. Figure 9 illustrated the effect of the number of specified loadings selected when the moment and z_r constraints are applied. For case 4 all eight loadings were used, with the specified area for the

eighth loading defined by the shaded area in figure 2. For case 5 the three loadings used in the method of reference 3 were applied: uniform, linear chordwise, and linear spanwise. Figure 9(b) indicates that the solution provided the requested z_r value for both cases, and the camber lines for case 4 are more reasonable than those for either case 5 or case 3. Figure 9(c) indicates that the drag for case 4 is substantially lower than that for case 5 and only slightly higher than that for case 3 (no z_r constraint).

Effect of modifying the minimum-drag root camber.- Since the root camber slopes for case 4 still are somewhat severe, the camber line at $\frac{y}{b/2} = 0.02$ was substituted at $\frac{y}{b/2} = 0$. The resulting design, designated case 6, is compared with the results for the unconstrained design (case 7) in figure 10. Case 6 is clearly superior to case 7 because the camber slopes are much less severe, pitching moment is zero at the design C_L (see fig. 10(b)), and the drag is only slightly higher. Therefore it appears that engineering judgment is justifiable in the wing design process. The modification method of substituting the $\frac{y}{b/2} = 0.02$ camber line at $\frac{y}{b/2} = 0$ is purely arbitrary and may not be the best method in this particular case.

Figure 11 summarizes the drag-due-to-lift factors for cases 3 to 7. Note that $C_D/C_{L,des}^2$ from the evaluation program is lower for case 6 than for case 4, indicating that the modification to the root chord was not detrimental.

Planform B

Wing planform B, shown in figure 12, represents a planform that might be employed on a highly maneuverable $M = 1.4$ airplane. The results of the design method applied at $M = 1.4$ to this planform serve to complement those obtained at $M = 3.5$ for planform A.

Example cases.- For planform B the design procedure was applied with and without the pitching-moment constraint for loadings 1 to 3 and loadings 1 to 7. Each application presented for wing planform B is denoted by a case number, as described in the following table:

Case	Description
1	Three loadings, design for given lift
2	Seven loadings, design for given lift
3	Three loadings, design for given lift and zero pitching moment
4	Seven loadings, design for given lift and zero pitching moment

The eighth loading and the z_r-constraint were not employed in this example, in order to present an application of the design method which differed from that used for planform A.

Moment reference location.- In order to exercise the pitching-moment constraint in a meaningful manner, the moment-center location of $0.662l$ was determined by performing a weight-and-balance analysis on a complete airplane configuration employing the wing planform of this example.

Effect of spanwise computation stations.- Figure 13 shows the variation of the drag-due-to-lift factor $C_D/C_{L,des}^2$ with number of spanwise computation stations. The circular symbols correspond to values obtained from the design procedure of this report; the square symbols were obtained by applying the evaluation procedure of reference 11 to the minimum-drag camber surface at the design lift coefficient. Results from the design program show no significant variation of drag-due-to-lift factor with number of spanwise computation stations; however, design-program and evaluation-program results are in best agreement for the maximum number of spanwise computation stations. The remaining discussion is predicated upon results obtained with 51 spanwise computation stations.

Effect of number of specified loadings and moment constraint.- The effect of number of loading distributions on the optimum lifting pressure distribution and the camber surface for a wing designed for given lift and no moment constraint is shown in figure 14. The lifting pressure distributions which correspond to the optimum combination of loadings are shown in figure 14(a). The paramount differences between the pressure distributions are in the complexity and the pressure gradients in the chordwise direction. The maximum pressure coefficient shown for seven loadings is over twice that obtained for three loadings; however, it is not known whether this type of loading distribution is practical. In order to assess the practicality of the more complex loading distribution it is necessary to select a particular wing thickness distribution and then consider the total combination of thickness and lifting pressures. Such consideration is beyond the scope of this report, and only lifting pressure distributions are presented here.

The camber surfaces shown in figure 14(b) have similar shapes except at $\frac{y}{b/2} = 0$. In this region the more complex loading distribution produces a camber surface which is also more complex but possesses a smaller overall z_c variation from leading to trailing edge. For conventional aircraft $\frac{y}{b/2} = 0$ is in the fuselage, and it is usually difficult to achieve substantial amounts of effective camber there; thus, the root-chord camber produced by seven loadings is more practical from this consideration.

For the wing designed for given lift and zero pitching moment, lifting pressure distributions and camber surfaces are shown in figure 15. A comparison of the camber surfaces in figure 15(b) again shows that the one corresponding to seven loadings has the smaller z_c difference between the leading and trailing edges of the root chord, but the camber-surface slopes dz_c/dx are much greater near the leading edge for seven loadings than for three loadings. These differences are reflected in the pressure distributions shown in figure 15(a).

For design lift coefficients of 0, 0.1, 0.2, and 0.3, minimum-drag wing camber surfaces were generated at $M = 1.4$ with and without moment constraints, employing three loadings and seven loadings. Each of these camber surfaces was evaluated by the method of reference 11, and the resulting aerodynamic coefficients of pitching moment and of drag due to lift are presented in figure 16 as functions of lift coefficient.

Aerodynamic coefficients for wing camber surfaces designed for given lift by using three loadings (case 1) and seven loadings (case 2) are presented in figures 16(a) and 16(b), respectively. The drag at the design lift is slightly lower for case 2 than for case 1; however, the pitching-moment characteristics are substantially different. At design lift, three loadings produced a wing camber surface which had a relatively large negative pitching moment. Trimming this moment out with a control surface would result in a trim drag increment in addition to the drag shown in figure 16(a). For this particular planform, the use of seven loadings without moment constraint essentially produced a self-trimming wing with a small positive moment at the design lift (unlike case 7 for planform A). Figures 16(c) and 16(d) show aerodynamic characteristics of wings designed for zero moment at given lift by wing three loadings (case 3) and seven loadings (case 4), respectively. All the twisted and cambered wings of figure 16 had better aerodynamic characteristics than the flat wing (i.e., design lift of zero) at the higher lift coefficients. Although the wings were designed for zero moment, application of the evaluation procedure resulted in moments near zero but not exactly zero. As previously explained, this discrepancy between the wing design and wing evaluation procedures is attributed to the numerical techniques employed in evaluating the camber-surface slopes. The lift-drag characteristics shown in figure 16(d) for case 4 are essentially the same as those shown in figure 16(b) for case 2 and in figure 16(c) for case 3.

The pitching-moment curves for case 2 are displaced somewhat in the positive direction as compared with the curves for the other cases in figure 16. In contrast to example A, the application of seven loadings with no pitching-moment constraint (case 2) produced an optimum wing possessing a small positive moment at the design lift coefficient. In this situation, constraining the pitching moment to be zero would not provide significant improvements in the moment characteristics and might even be detrimental to the lift-drag characteristics. These two examples clearly illustrate that the benefits to be gained by use of the various options provided with the design program are dependent on the planform.

The drag-due-to-lift factor, which serves as a measure of the wing efficiency, is summarized in figure 17 for the four cases of planform B. In all cases the drag-due-to-lift factors obtained from the evaluation program are larger than those obtained from the design program. The factors are smaller for seven loadings than for three loadings, and for three loadings the addition of the moment constraint results in an increase in drag-due-to-lift factor, but for seven loadings the drag-due-to-lift factors are the same.

Possible Extensions

Although the present design method has been applied only to a wing alone, it should be applicable to multiple lifting surfaces such as wing-tail and wing-canard combinations. The evaluation capability for wing-tail and wing-canard combinations exists and has been successfully demonstrated (ref. 11); similar success is anticipated for the design of these combinations. The significance of such a design capability can be appreciated by noting that the usual procedure is to design an optimum wing and then add a horizontal tail in order to trim the configuration. However, if a separate control surface is to be used in combination with a wing, the most direct procedure for arriving at an optimum combination would be to incorporate the control-surface effects into the initial wing design process.

This approach solves the complex problem of determining how much trim moment should be obtained from wing twist and camber and how much from the control surface. This type of solution also determines whether the lift on the control surface should be positive or negative for a given center-of-gravity position.

CONCLUSIONS

A numerical method based on linearized theory has been developed and programed for the CDC 6600 computer to design a minimum-drag supersonic-wing camber surface of arbitrary planform for a given lift, with options for constraining the pitching moment and/or the surface deformation at the trailing edge of the root chord and for selecting any desired combination of eight specified wing-loading distributions to be employed in the optimization procedure. The application of this method to two examples led to the following conclusions:

1. For the two wing planforms investigated, the drag penalties for designing wings to be self-trimming and to have a reasonable camber surface are relatively small.

2. The use of seven and eight loadings consistently produced camber surfaces having lower drag than camber surfaces produced by three loadings.

3. The benefits obtained by using constraints on the pitching moment and the root-chord trailing-edge ordinate are dependent on the planform.

4. The number of spanwise computation stations required for a valid solution is dependent on the number of specified loadings used.

5. Replacing the wing-root camber line computed by the program with a camber line from the adjacent outboard span station does not significantly alter the drag and can provide a more reasonable camber surface.

Langley Research Center,
National Aeronautics and Space Administration,
Hampton, Va., November 20, 1972.

APPENDIX A

INPUT DATA

The purpose of this appendix is to provide a description of the input required for the computer program. All input is in NAMELIST format (ref. 12). A description of the required inputs and the FORTRAN variables used by the computer program are as follows:

FORTRAN Variable	Description
	One card of Hollerith identifying information
$INPUT	Arbitrary name required by the loading routine to define first input-data block
XM	Free-stream Mach number
XMAX	Largest value of x in wing definition
JBYMAX*	Total number of spanwise stations for camber-surface computation (JBYMAX $\leqq$ 51)
JBYS(1)*	Table of spanwise stations for camber-surface computation, integer values (0 $\leqq$ JBYS $\leqq$ NON)
NON*	Number of semispan grid elements selected to represent wing (NON $\leqq$ 100)
XLEO	x-coordinate of wing leading edge at y = 0
XTEO	x-coordinate of wing trailing edge at y = 0
RATIO	Factor used to proportion z_c-ordinates for given design lift coefficient $\left(\frac{C_{L,des}\beta(b/2)}{NON}\right)$
NOM*	Number of Mach numbers other than XM
REFAR	Reference area of wing

FORTRAN Variable	Description
SPAN	Total span of wing
ICG*	Selection for moment constraint (ICG = 1 to exercise moment constraint, input XCG)
XCG	x-distance from XLEO to pitching-moment center
IZREST*	Selector for z_r constraint (IZREST = 1 to exercise z_r constraint, input ZMIN)
ZMIN	z-distance from horizontal reference plane to trailing edge of root chord (z_r)
LOAD1*	Selector for loading 1 (LOAD1 = 1 applies uniform loading)
LOAD2*	Selector for loading 2 (LOAD2 = 1 applies linear chordwise loading)
LOAD3*	Selector for loading 3 (LOAD3 = 1 applies linear spanwise loading)
LOAD4*	Selector for loading 4 (LOAD4 = 1 applies quadratic spanwise loading)
LOAD5*	Selector for loading 5 (LOAD5 = 1 applies parabolic chordwise loading)
LOAD6*	Selector for loading 6 (LOAD6 = 1 applies quadratic chordwise loading)
LOAD7*	Selector for loading 7 (LOAD7 = 1 applies cubic chordwise loading)
LOAD8*	Selector for loading 8 (LOAD8 = 1 applies a linear chordwise loading on the specified area)

FORTRAN Variable	Description
APUNCH	Variable to control punch output. APUNCH = 0. for no punch output, APUNCH = 1. to punch z_c-ordinates in format (4(E18.8,1H)) compatible with input to program D2340, APUNCH = 2. to punch z_c-ordinates in format (10(F7.3),2X,5HTZORD,I2) compatible with input to D2500 wave-drag program, APUNCH = 3. to punch z_c-ordinates in both of the above formats.
APLOT	Variable to control plotting of wing camber. APLOT = 0. for no plots, APLOT = 1. to request plots.
TMACH(1)	Table of other Mach numbers corresponding to NOM
TXLE(1)	Table of x-coordinates of wing leading edge at successive span stations of $y = \frac{(b/2)N}{NON}$ where N = 1 to NON; used only when TYPEX = 0.
TXTE(1)	Table of x-coordinates of wing trailing edge at successive span stations of $y = \frac{(b/2)N}{NON}$ where N = 1 to NON; used only when TYPEX = 0.
TYPEX	If TYPEX = 0. input TXLE and TXTE tables and omit remaining input variables in this data block; if TYPEX = 1. TXLE and TXTE tables will be generated from the following input information
NLEX*	Number of leading-edge definition points (≦50)
NTEX*	Number of trailing-edge definition points (≦50)
TBLEX(1)	Table of NLEX wing leading-edge x-coordinates
TBLEY(1)	Table of NLEX wing leading-edge y-coordinates
TBTEX(1)	Table of NTEX wing trailing-edge x-coordinates
TBTEY(1)	Table of NTEX wing trailing-edge y-coordinates
$	Denotes end of input-data block

The following input-data block is required when applying loading 8 (i.e., LOAD 8 = 1).

FORTRAN Variable	Description
$INPT8	Arbitrary name required by the loading routine to define second input-data block
XLEOLOD	x-coordinate of specified-area leading edge at $y = 0$
TXLOAD(1)	Table of x-coordinates of specified-area leading edge at successive span stations of $y = \frac{(b/2)N}{NON}$ where $N = 1$ to NON; used only when TYPEX = 0.
NX8*	Number of leading-edge definition points describing specified area (≤50); TYPEX = 1.
TBX8(1)	Table of NX8 x-coordinates at specified-area leading edge
$	Denotes end of input-data block
*	Fixed-point number

APPENDIX B

OUTPUT DATA

The input data, in real dimensions, are printed out. All other dimensional output numbers are in program dimensions (multiplied by NON/β(b/2)) except those multiplied by RATIO. The input data in program dimensions are next printed out along with the pressure-coefficient terms for the eight loadings:

CPU — Lifting pressure coefficient of uniform load = 1.0

DCPDBY — Lifting pressure coefficient of linear spanwise loading per unit $\beta y = 0.04$

DCPDXP — Lifting pressure coefficient of linear chordwise loading per unit $x' = 0.04$

DCPDBY2 — lifting pressure coefficient of parabolic spanwise loading per unit $\beta^2 y^2 = 0.04$

DCPDX5 — Lifting pressure coefficient of parabolic chordwise loading per unit $(x')^2 = 0.0004$

DCPDX6 — Lifting pressure coefficient of quadratic chordwise loading per unit $(x')(x' - c) = 0.0016$

DCPDX7 — Lifting pressure coefficient of cubic chordwise loading per unit $(x')^2(1.5c - x') = 0.00008$

DCPDX8 — Lifting pressure coefficient of linear chordwise loading per unit x' on the specified area = 0.04

The drag coefficients of interference between each loading on the camber surface and the other loadings are next printed, along with the following values for each loading:

AREA — Right-hand wing area, $\int_0^{b/2} c\, dy$

CBAR — Wing mean aerodynamic chord, $\int_0^{b/2} c^2 dy/\text{AREA}$

CD Wing drag coefficient, $\int_0^{b/2}(CDS)c\,dy/AREA$

CL Wing lift coefficient, $\int_0^{b/2}(CLS)c\,dy/AREA$

CMCG Wing pitching-moment coefficient about XCG, $\int_0^{b/2}(CMS)c^2dy/AREA(CBAR)$

The force coefficients of the specified and interference loadings are printed with other terms related to the solution of the simultaneous equations:

CDij Drag coefficient of interference between loadings i and j (see eq. (20) of ref. 3)

CLi Lift coefficient of ith loading

DETERM Value of the determinant of the coefficient matrix used in solving equations (3)

Ai Proportionality factor for ith loading to produce minimum-drag combination having total lift coefficient of 1.0

LAMBDA1 λ_L of simultaneous equations (C_L constraint)

LAMBDA2 λ_m of simultaneous equations (moment constraint)

LAMBDA3 λ_z of simultaneous equations (z constraint)

The wing data for the minimum-drag loading are printed for each semispan station selected (see JBYS(1) in appendix A). The calculated ZRATIO values are interpolated at standard NACA chordwise stations.

YB2 Semispan station

XRATIO x-distance to the center of the grid element times RATIO

L x-distance to trailing edge of grid element

DZDX	Streamwise camber-surface slope at x or x', $\partial z_c/\partial x$
ZRATIO	z_c times RATIO, value of camber surface ordinate at x or x', RATIO $\int_0^{x'}\left(\frac{\partial z_c}{\partial x}\right)dx'$
LSTAR	Grid element number, ascending order in x-direction
CP/CL	Lifting pressure coefficient at trailing edge of grid element divided by wing lift coefficient
XPOC	x' expressed as fraction of local chord, x'/CHORD
CHORD	Chord length at selected YB2, $(TXTE - TXLE)_{JBYS} = c$
CDS	Section axial-force coefficient at selected YB2, $-\int_0^1 \Delta C_p \frac{\partial z_c}{\partial x} d\left(\frac{x'}{c}\right)$
CLS	Section lift coefficient at selected YB2, $\int_0^1 \Delta C_p \, d\left(\frac{x'}{c}\right)$
CMS	Section pitching-moment coefficient about XCG, $-\int_0^1 \Delta C_p \frac{x - XCG}{c} d\left(\frac{x'}{c}\right)$

The drag-due-to-lift factor (CD/CL**2) based on REFAR, and the values of AREA, CBAR, CD, CL, and CMCG for the minimum-drag wing, are printed last.

REFERENCES

1. Grant, Frederick C.: The Proper Combination of Lift Loadings for Least Drag on a Supersonic Wing. NACA Rep. 1275, 1956. (Supersedes NACA TN 3533.)

2. Brown, Clinton E.; and McLean, Francis E.: The Problem of Obtaining High Lift-Drag Ratios at Supersonic Speeds. J. Aero/Space Sci., vol. 26, no. 5, May 1959, pp. 298-302.

3. Carlson, Harry W.; and Middleton, Wilbur D.: A Numerical Method for the Design of Camber Surfaces of Supersonic Wings With Arbitrary Planforms. NASA TN D-2341, 1964.

4. Robins, A. Warner; Morris, Odell A.; and Harris, Roy V., Jr.: Recent Research Results in the Aerodynamics of Supersonic Vehicles. J. Aircraft, vol. 3, no. 6, Nov.-Dec. 1966, pp. 573-577.

5. Carlson, Harry W.: Aerodynamic Characteristics at Mach Number 2.05 of a Series of Highly Swept Arrow Wings Employing Various Degrees of Twist and Camber. NASA TM X-332, 1960.

6. McLean, F. Edward; and Fuller, Dennis E.: Supersonic Aerodynamic Characteristics of Some Simplified and Complex Aircraft Configurations Which Employ Highly Swept Twisted-and-Cambered Arrow-Wing Planforms. Vehicle Design and Propulsion. American Inst. Aeron. and Astronautics, Nov. 1963, pp. 98-103.

7. Morris, Odell A.; and Fournier, Roger H.: Aerodynamic Characteristics at Mach Numbers 2.30, 2.60, and 2.96 of a Supersonic Transport Model Having a Fixed, Warped Wing. NASA TM X-1115, 1965.

8. Sokolnikoff, I. S.; and Redheffer, R. M.: Mathematics of Physics and Modern Engineering. Second ed., McGraw-Hill Book Co., Inc., c.1966.

9. Margason, Richard J.; and Lamar, John E.: Vortex-Lattice FORTRAN Program for Estimating Subsonic Aerodynamic Characteristics of Complex Planforms. NASA TN D-6142, 1971.

10. Huffman, Jarrett K.: Effects of Wing Pivot Location and Forewing Configuration on the Low-Speed Aerodynamic Characteristics of a Variable-Sweep Airplane Model. NASA TM X-2674, 1972.

11. Middleton, Wilbur D.; and Carlson, Harry W.: Numerical Method of Estimating and Optimizing Supersonic Aerodynamic Characteristics of Arbitrary Planform Wings. J. Aircraft, vol. 2, no. 4, July-Aug. 1965, pp. 261-265.

12. Anon.: Control Data 6400/6500/6600 Computer Systems FORTRAN Reference Manual. Publ. No. 60174900, Control Data Corp.

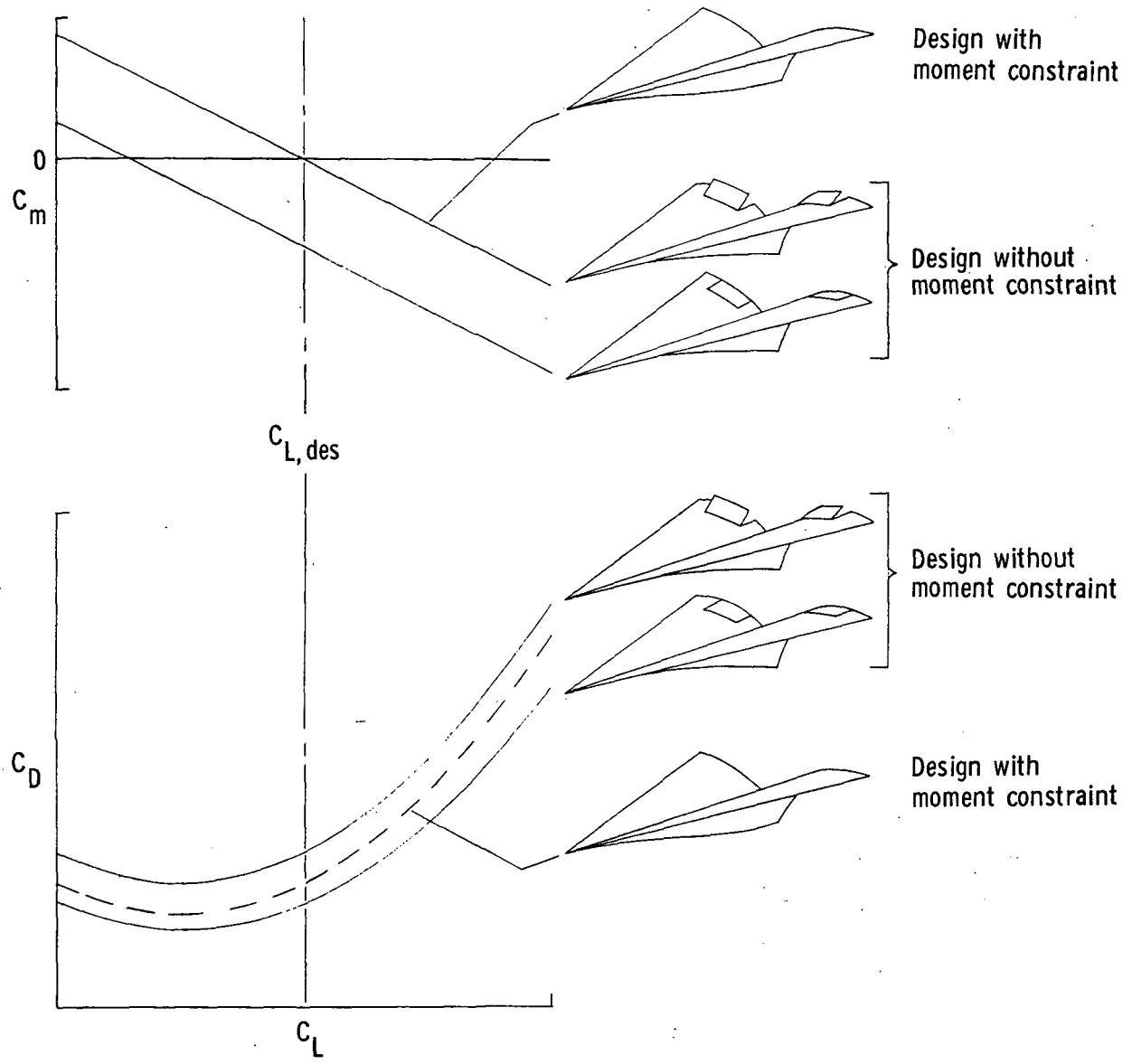

Figure 1.- Potential use of wing twist and camber to reduce trim drag.

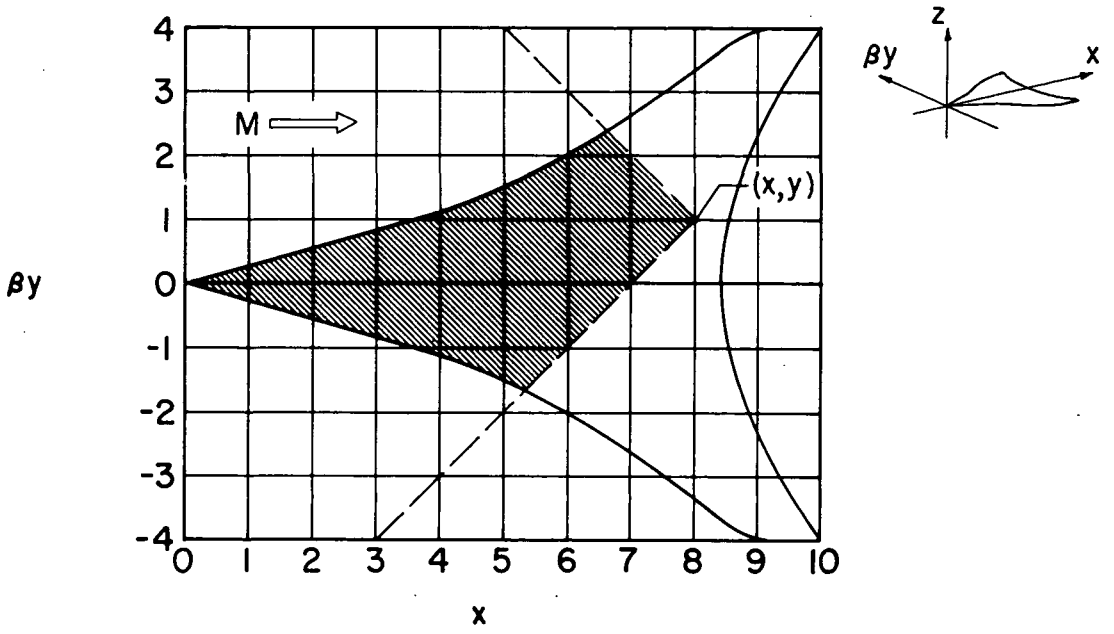

Figure 2.- Cartesian coordinate system.

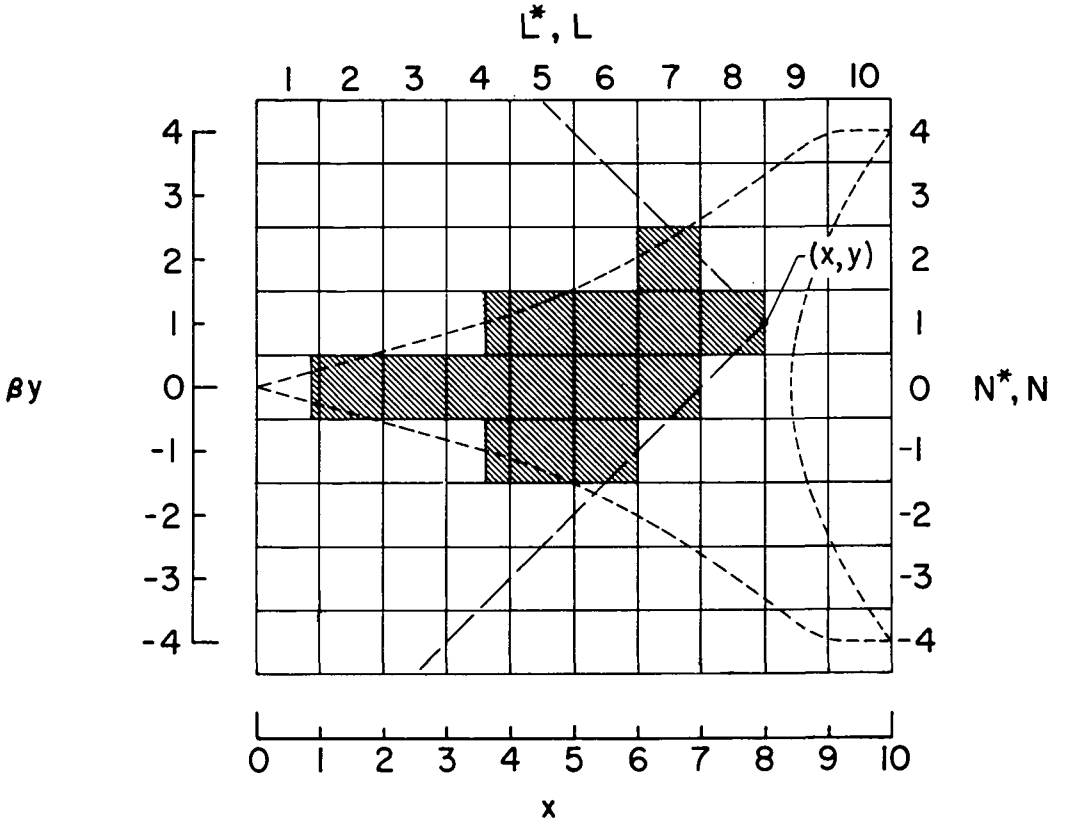

Figure 3.- Grid system used in numerical solution.

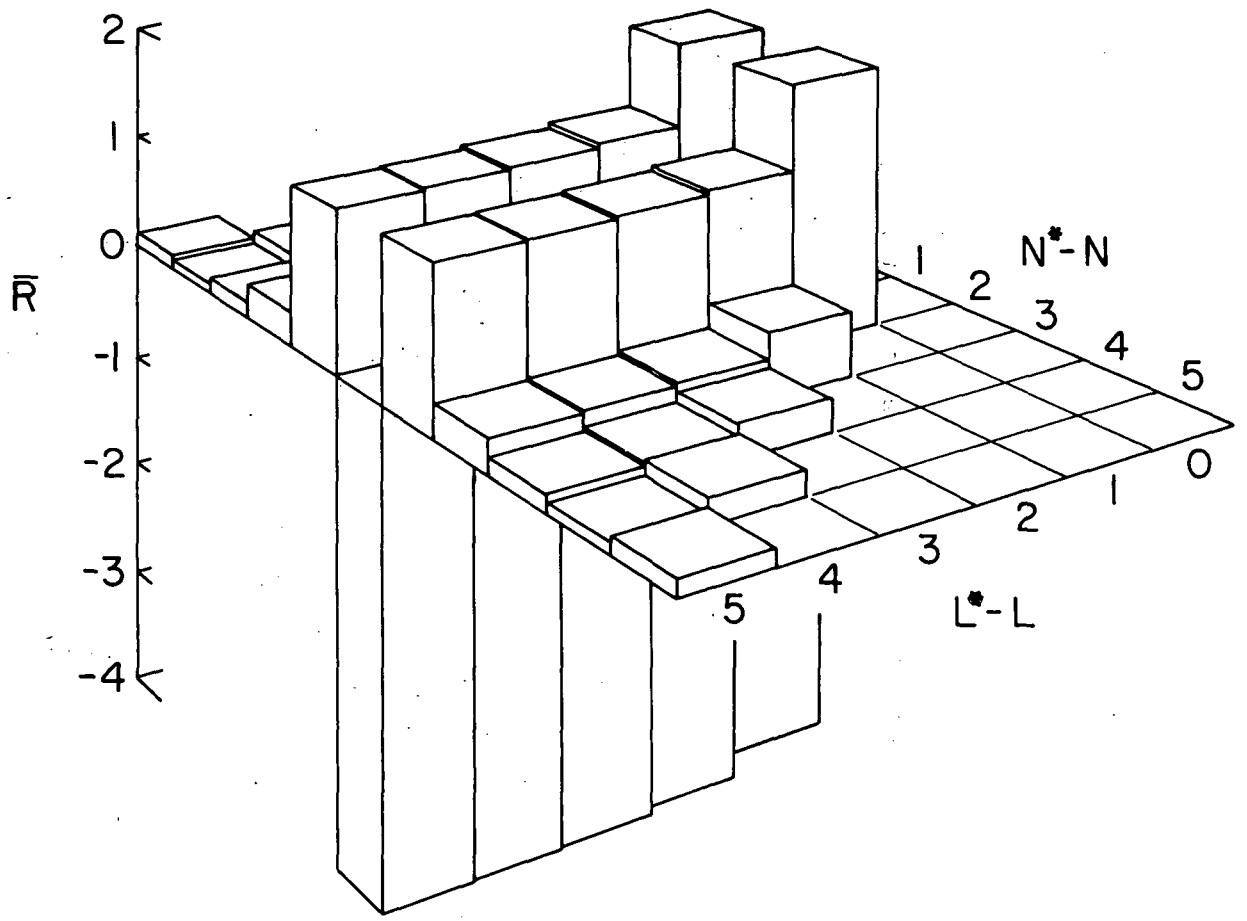

Figure 4.- Influence function $\bar{R}$.

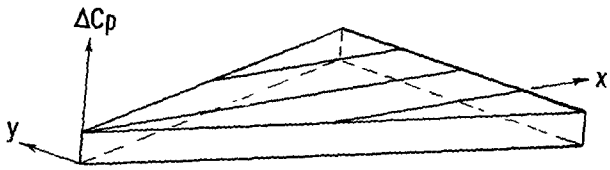

Uniform Loading
No. 1

Linear Chordwise Loading
No. 2

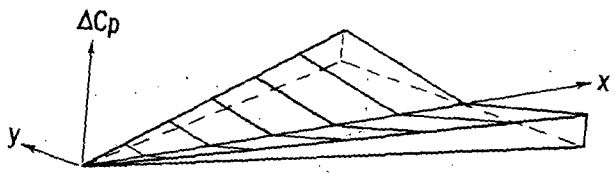

Linear Spanwise Loading
No. 3

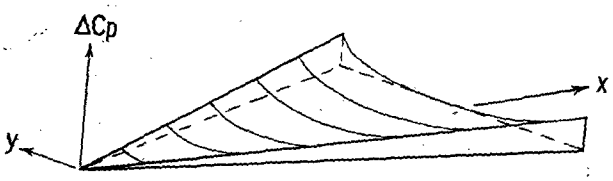

Quadratic Spanwise Loading
No. 4

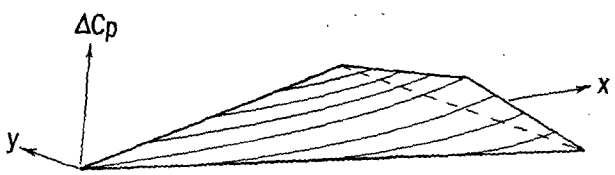

Parabolic Chordwise Loading
No. 5

Quadratic Chordwise Loading
No. 6

Cubic Chordwise Loading
No. 7

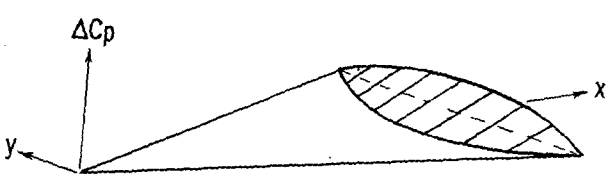

Linear Chordwise Loading
on Specified Area
No. 8

Figure 5.- Schematic drawings of the eight specified loadings.

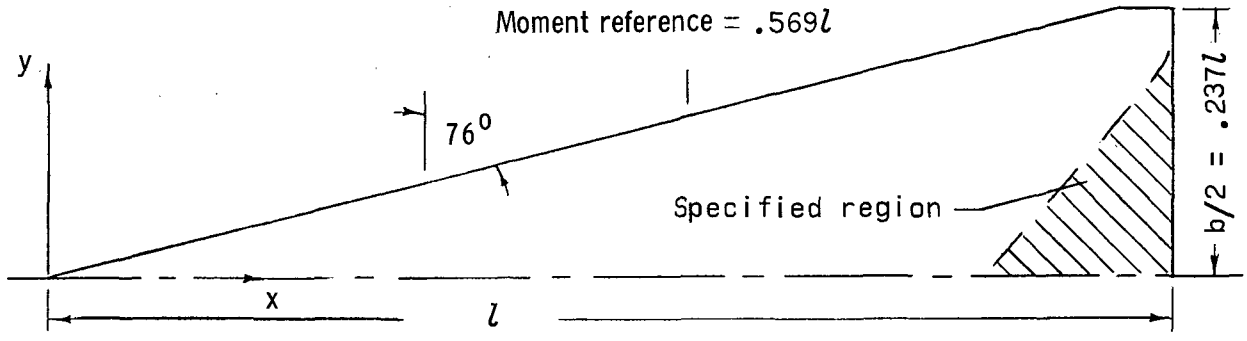

Figure 6.- Wing planform A.

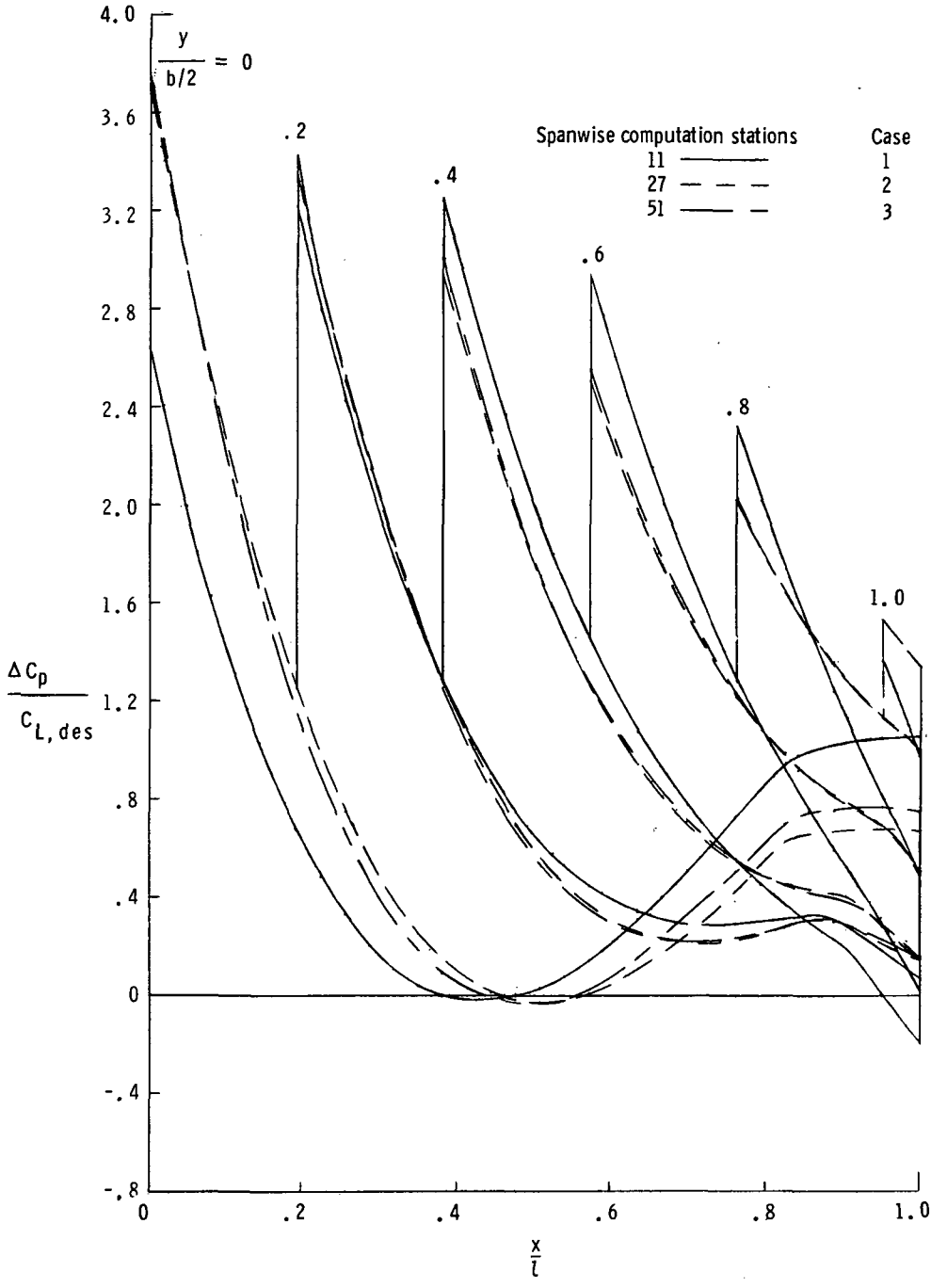

(a) Lifting pressure distributions.

Figure 7.- Effect of number of spanwise computation stations on design of planform A wings with moment constraint and no z_r constraint for eight loadings. M = 3.50.

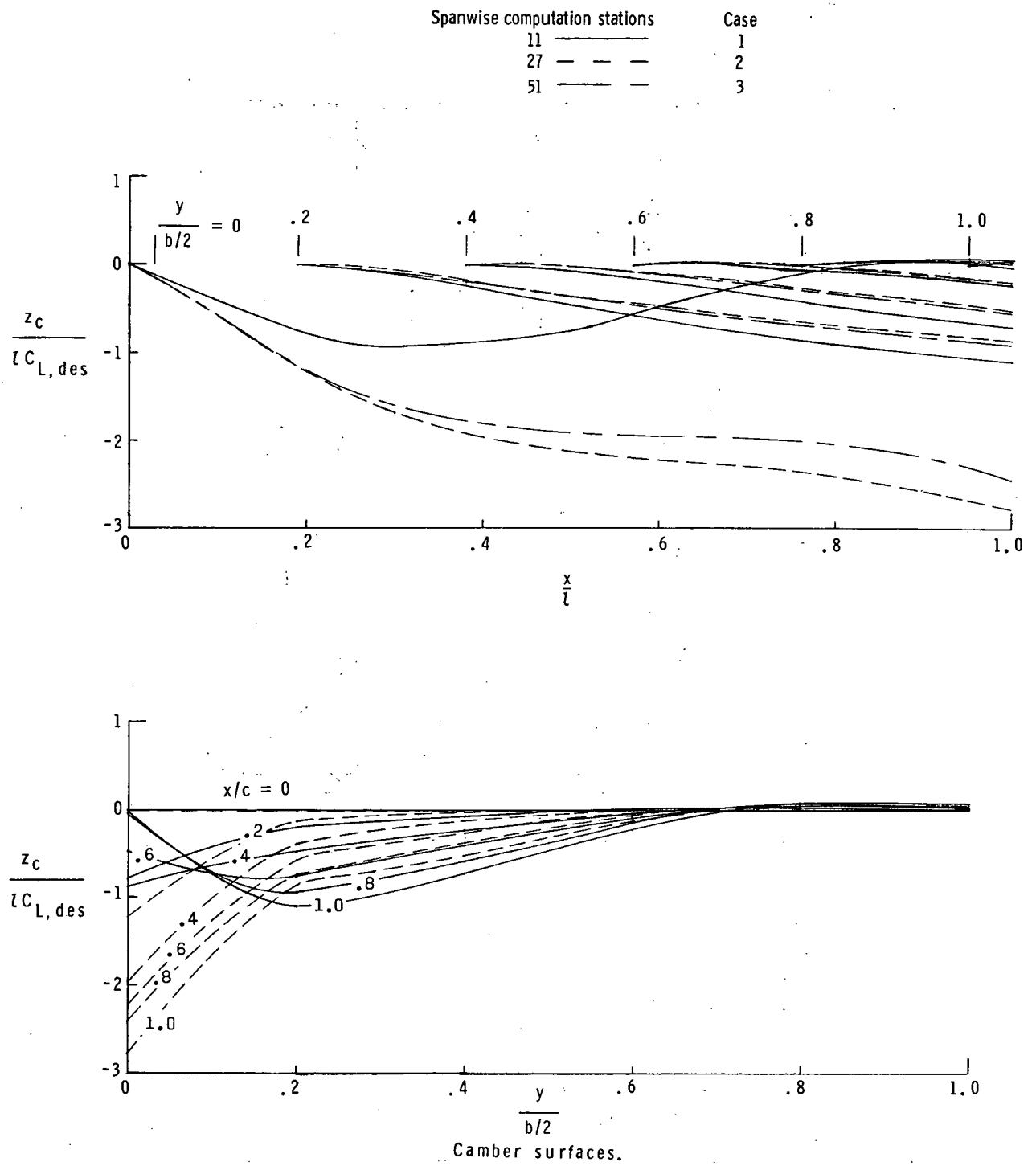

(b) Camber surfaces.

Figure 7.- Continued.

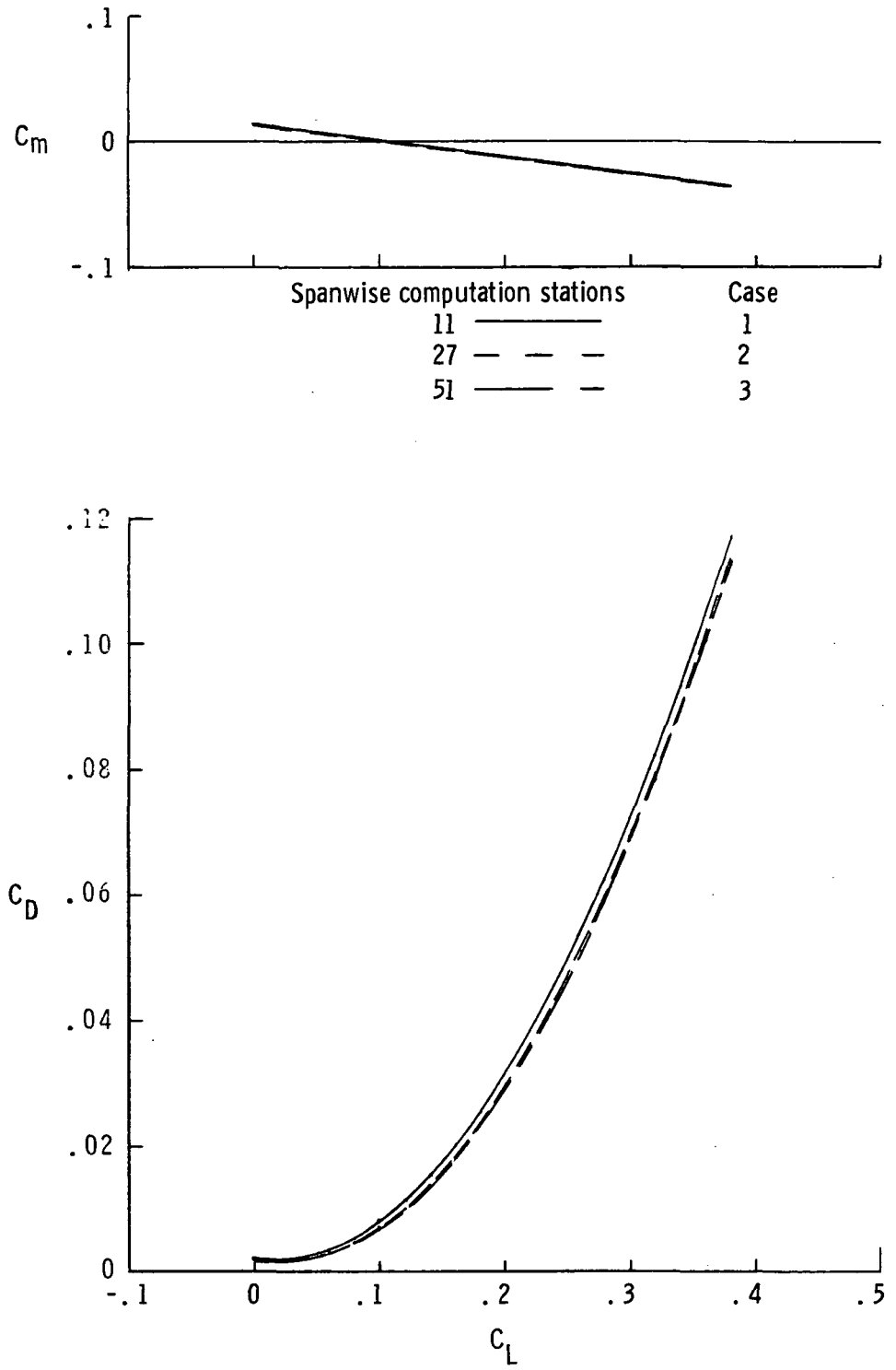

(c) Longitudinal aerodynamic characteristics as determined by evaluation program. $C_{L,des} = 0.10$.

Figure 7.- Concluded.

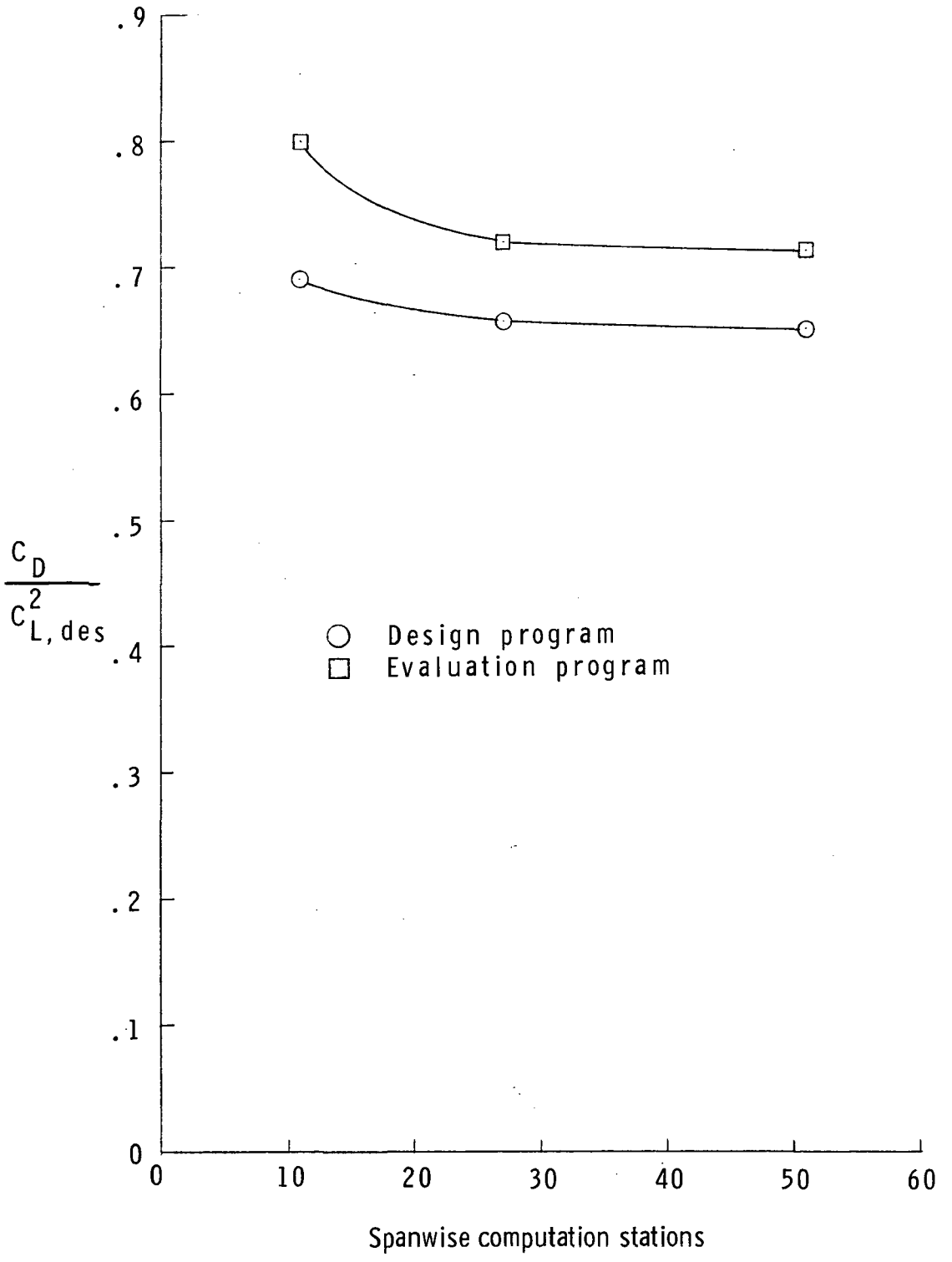

Figure 8.- Variation of drag-due-to-lift factor with number of spanwise computation stations for planform A wing.

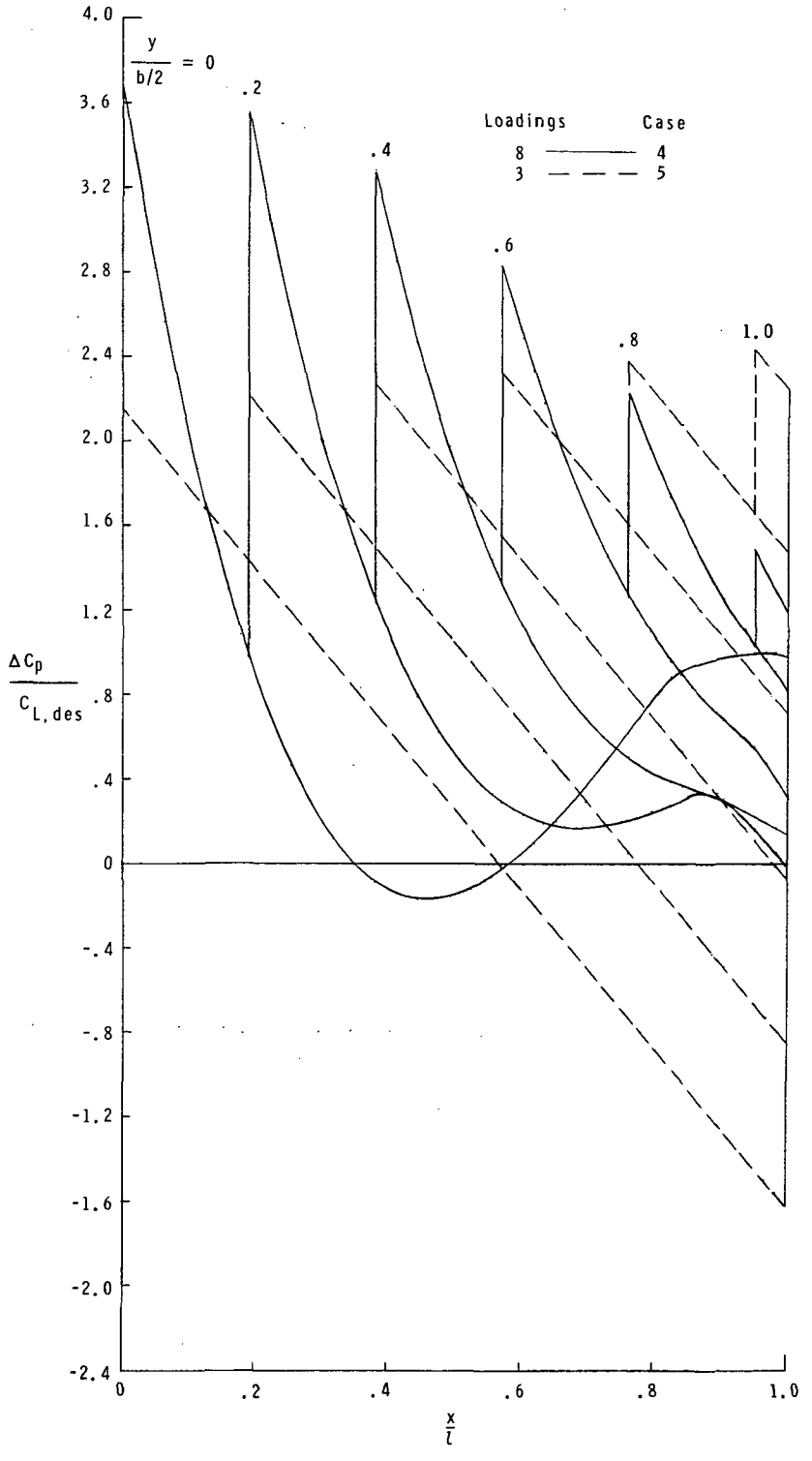

(a) Lifting pressure distributions.

Figure 9.- Effect of number of specified loadings on design of planform A wing with moment and z_r constraint. $z_r = -1.27\ell C_{L,des}$; M = 3.50.

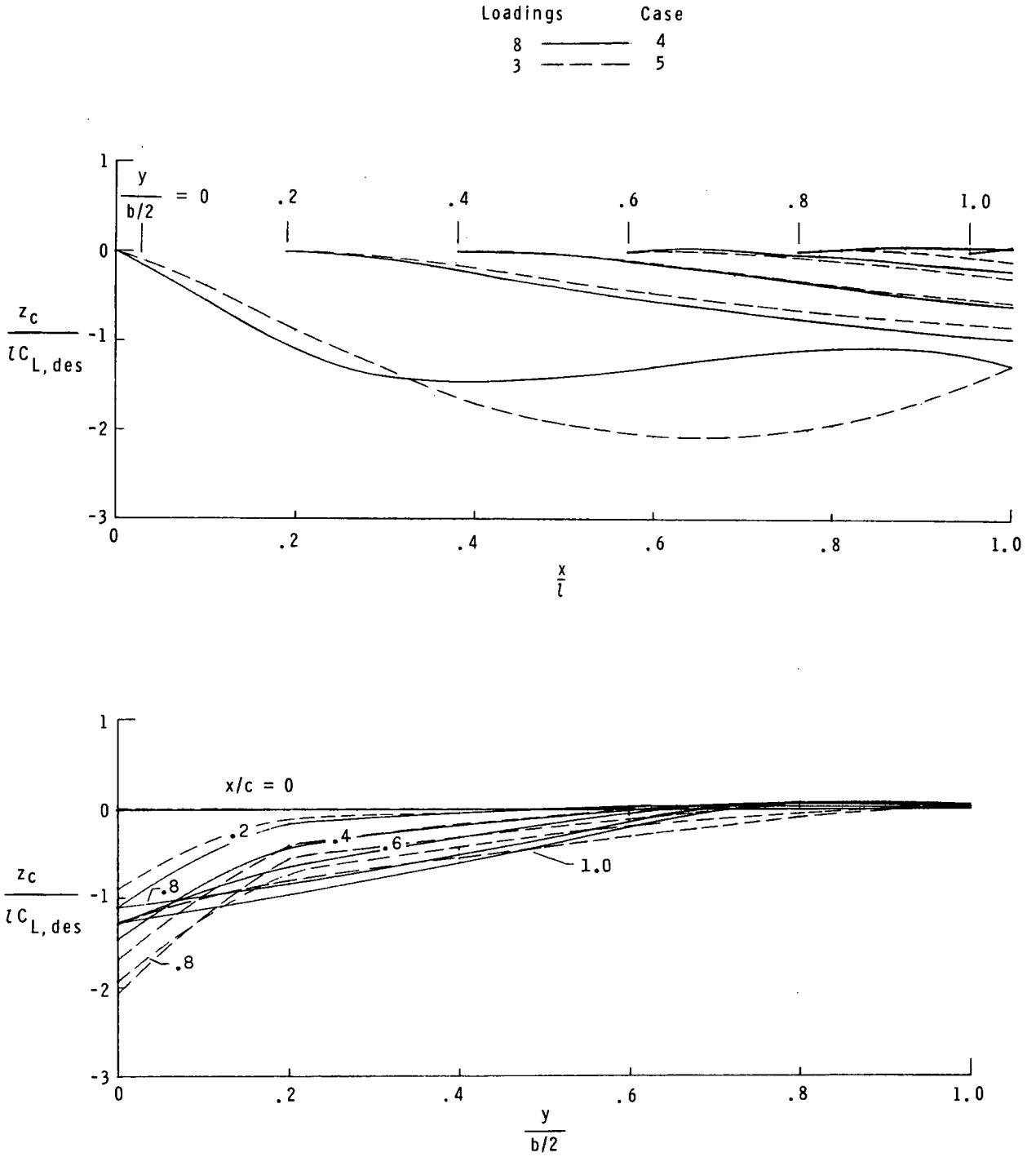

(b) Camber surfaces.

Figure 9.- Continued.

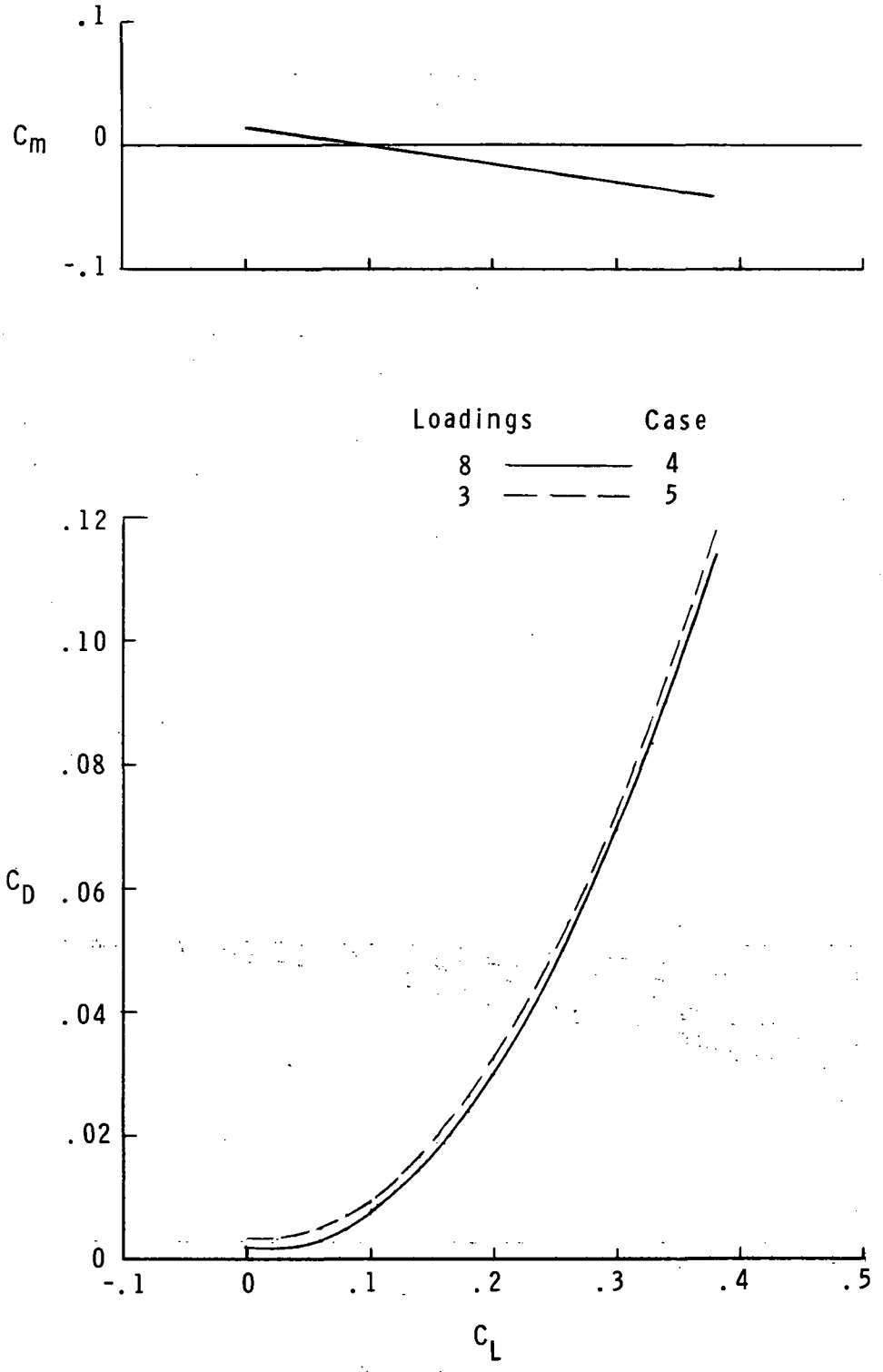

(c) Longitudinal aerodynamic characteristics as determined by evaluation program. $C_{L,des} = 0.10$.

Figure 9.- Concluded.

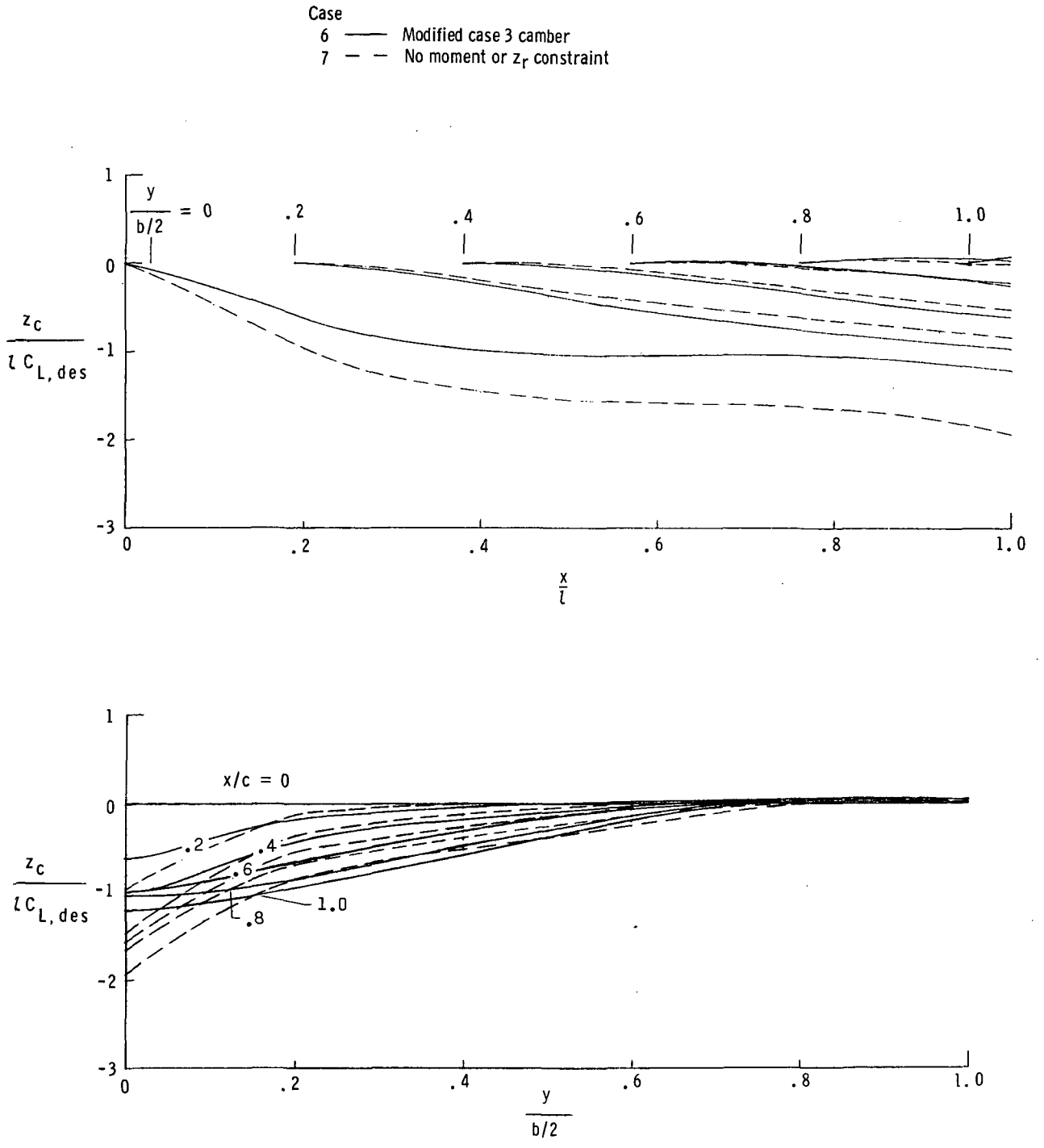

(a) Camber surfaces.

Figure 10.- Comparison of modified case 3 with unconstrained design case of planform A wings for eight loadings. M = 3.50.

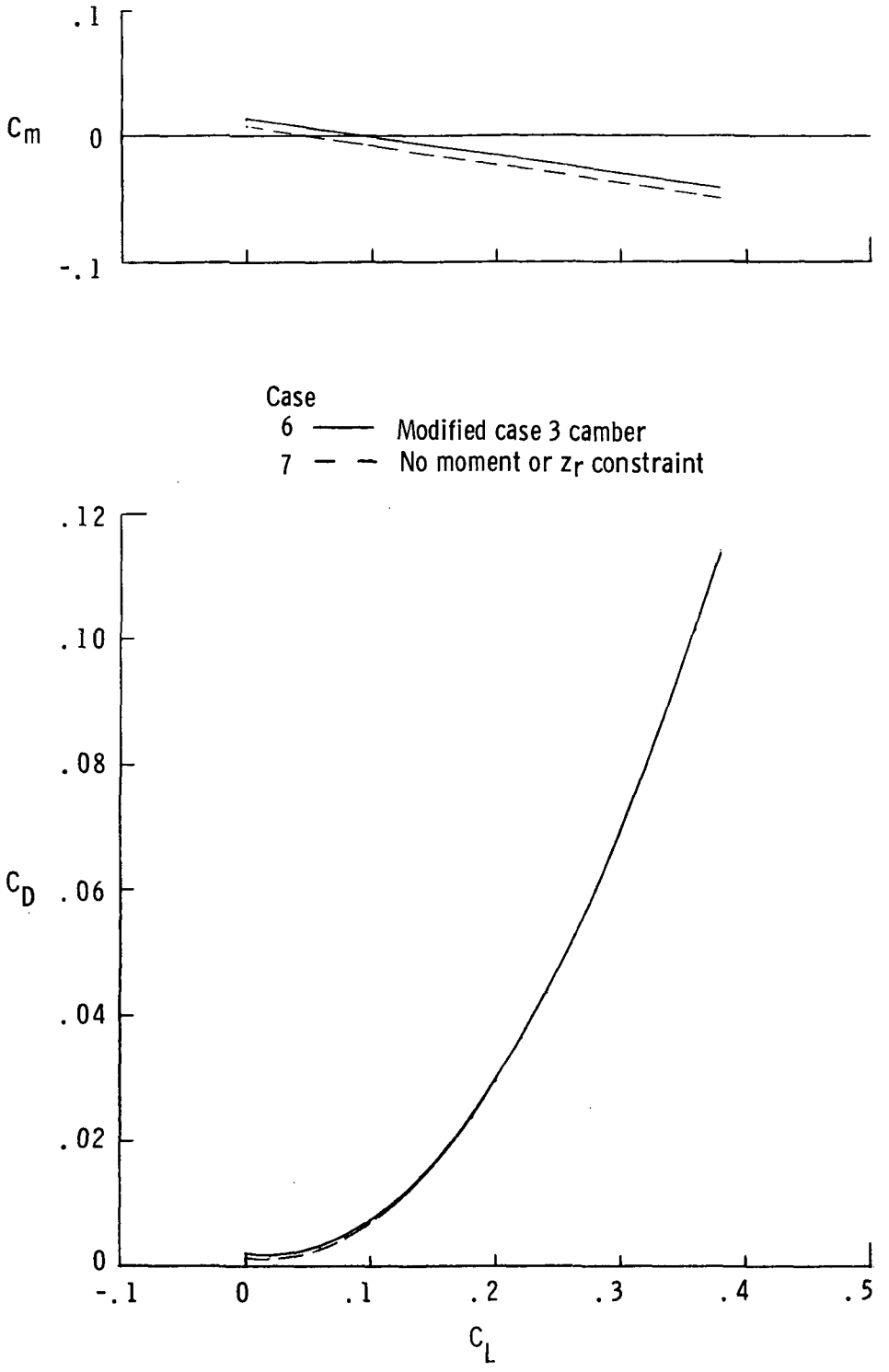

(b) Longitudinal aerodynamic characteristics as determined by evaluation program. $C_{L,des} = 0.10$.

Figure 10.- Concluded.

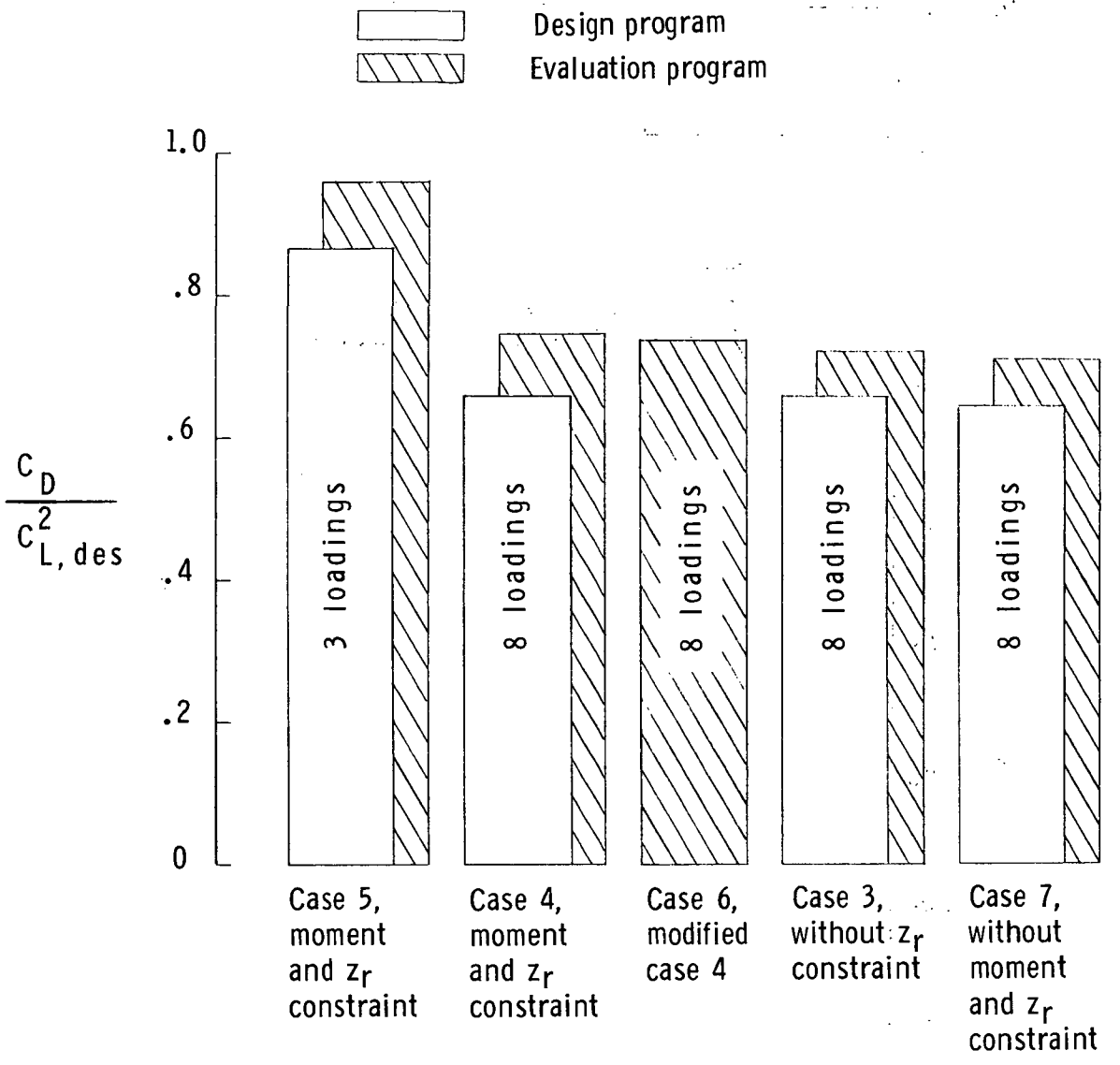

Figure 11.- Summary of effect of design program options on drag-due-to-lift factor for planform A wings.

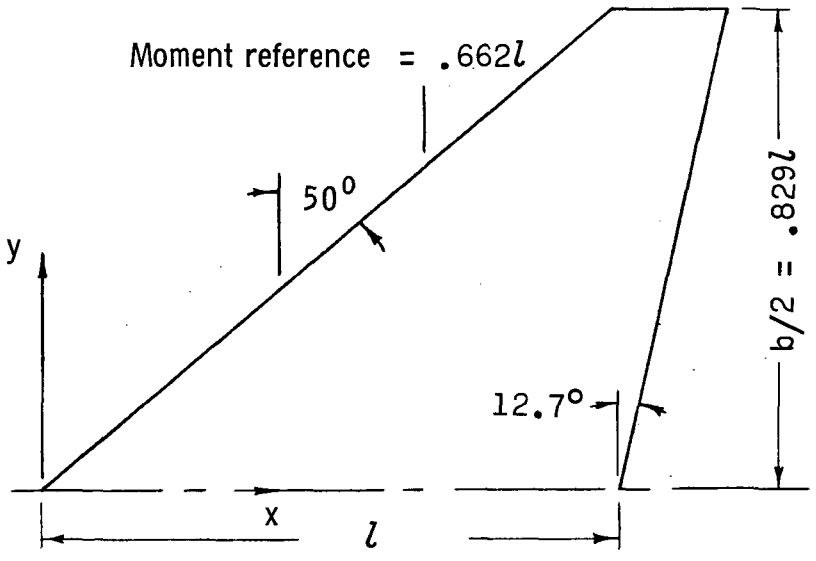

Figure 12.- Wing planform B.

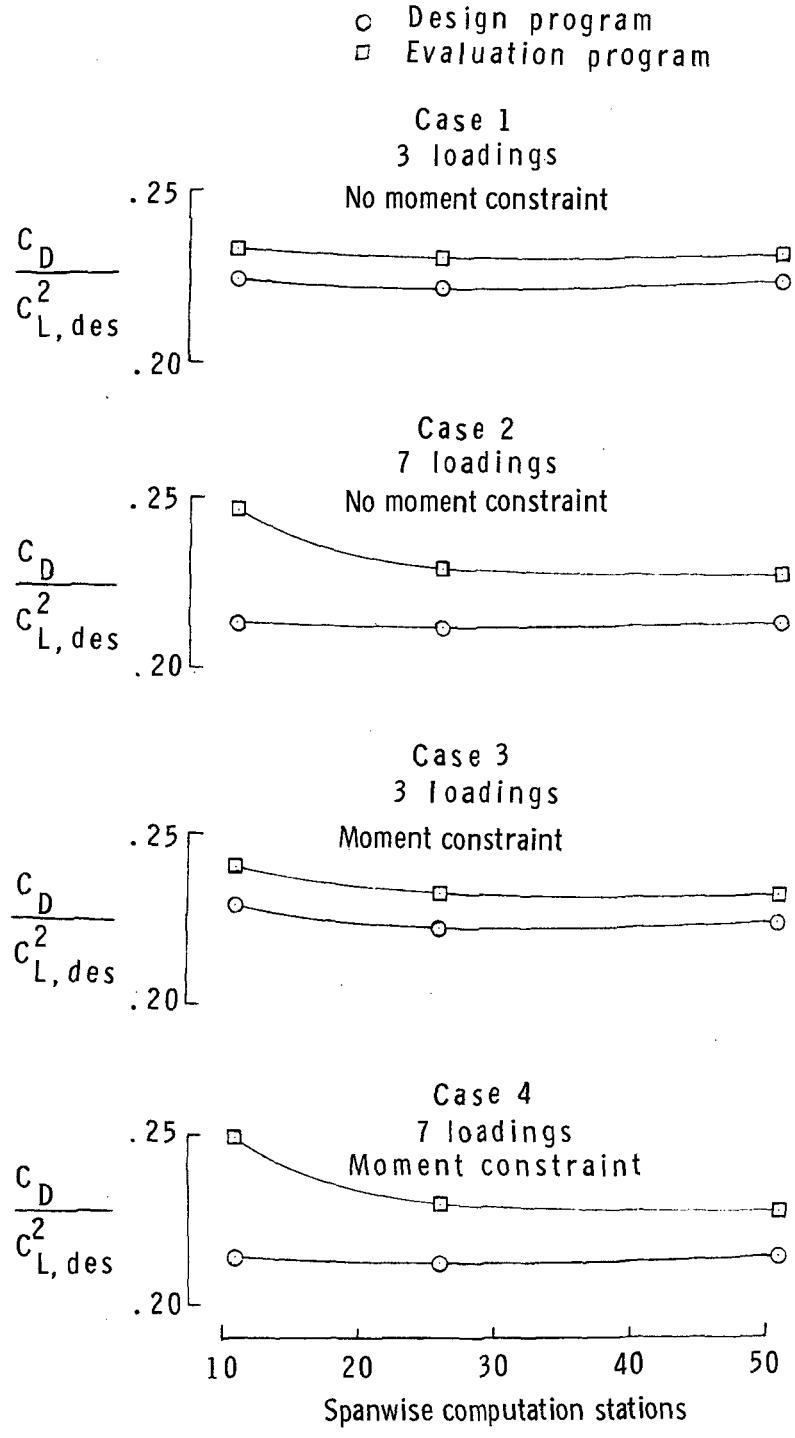

Figure 13.- Variation of drag-due-to-lift factor with number of spanwise computation stations for planform B wings.

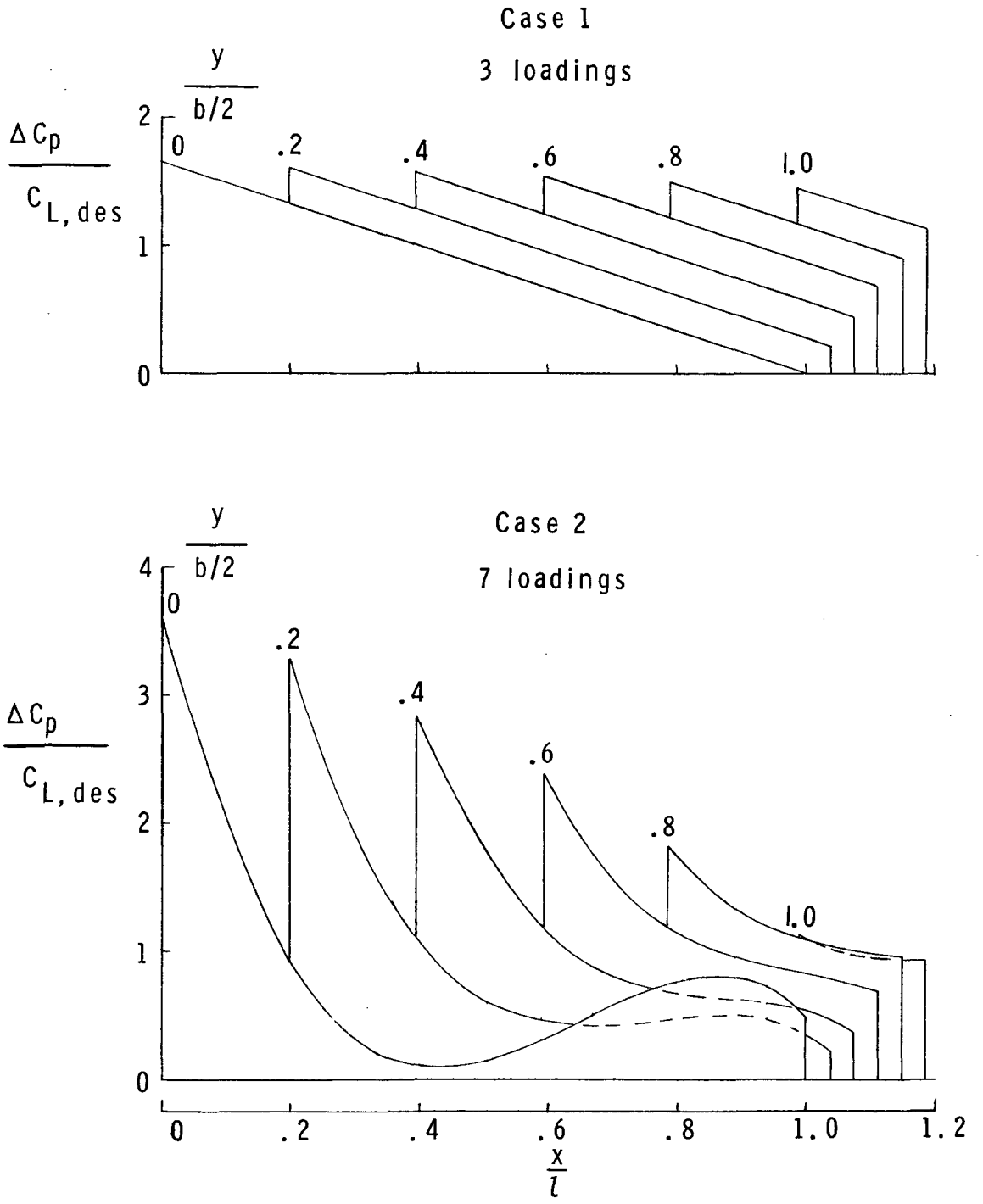

(a) Lifting pressure distributions.

Figure 14.- Effect of number of specified loadings on design of planform B wings for given lift without moment constraint. M = 1.4.

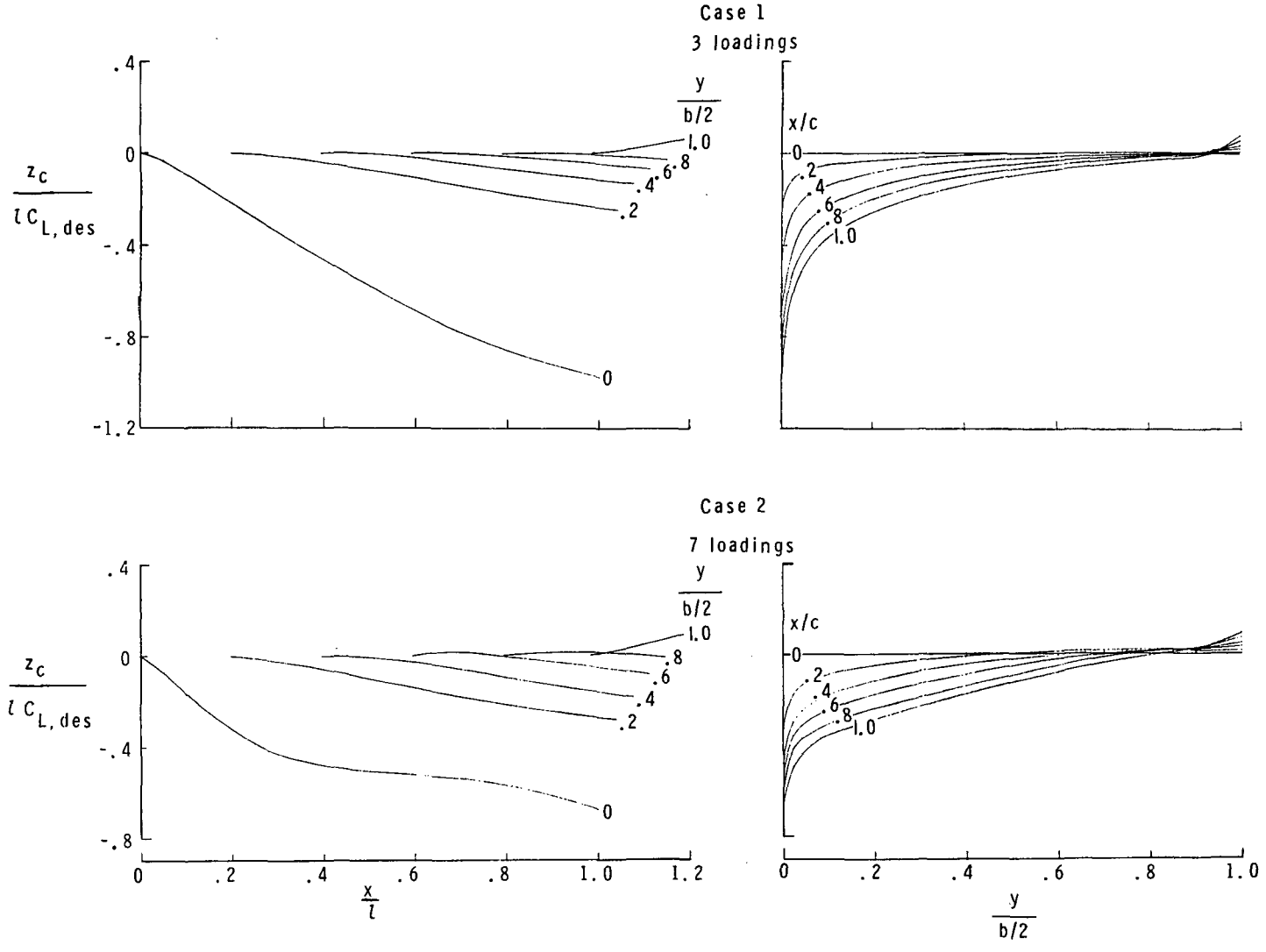

(b) Camber surfaces.

Figure 14.- Concluded.

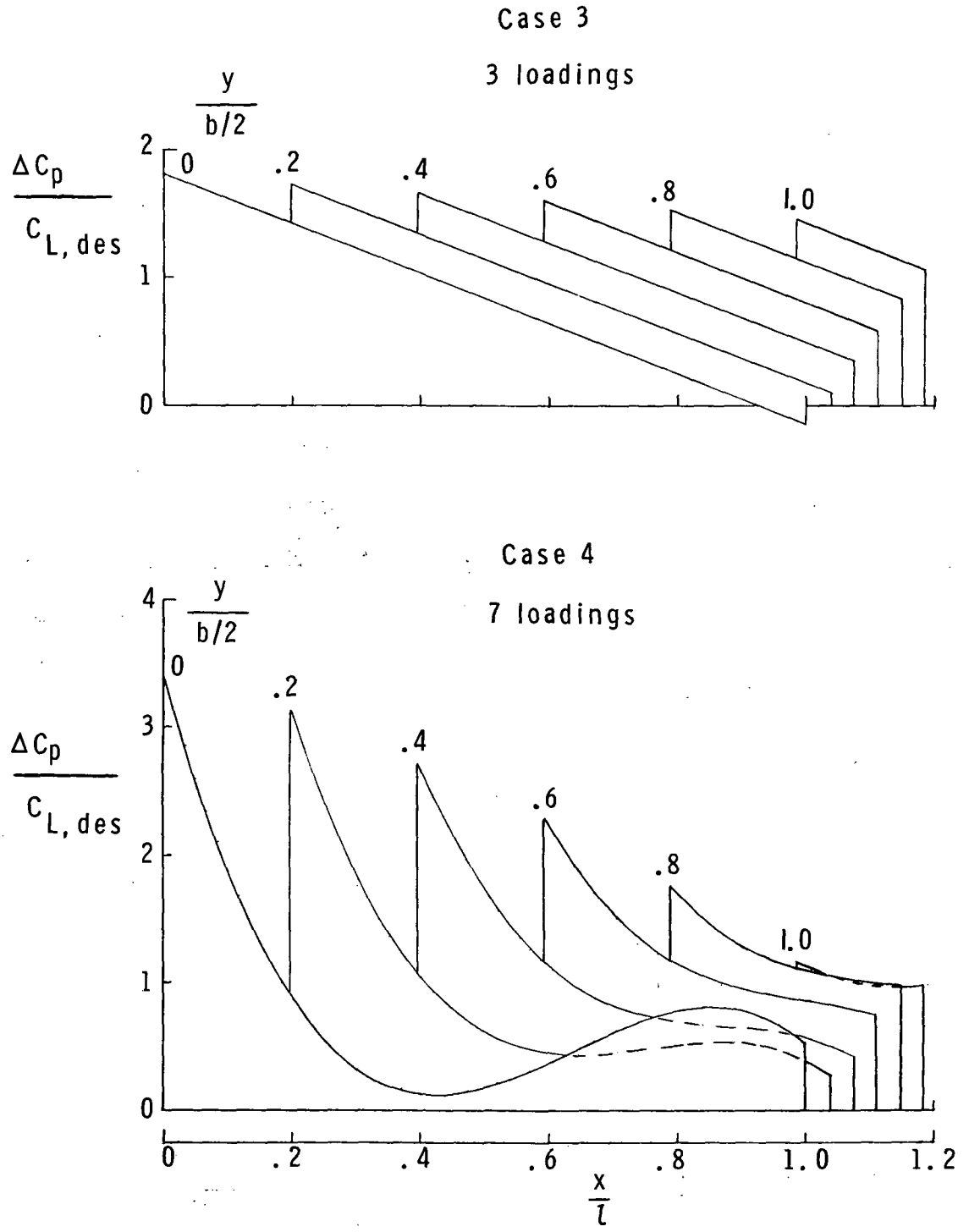

(a) Lifting pressure distributions.

Figure 15.- Effect of number of specified loadings on design of planform B wings for given lift with moment constraint. M = 1.4.

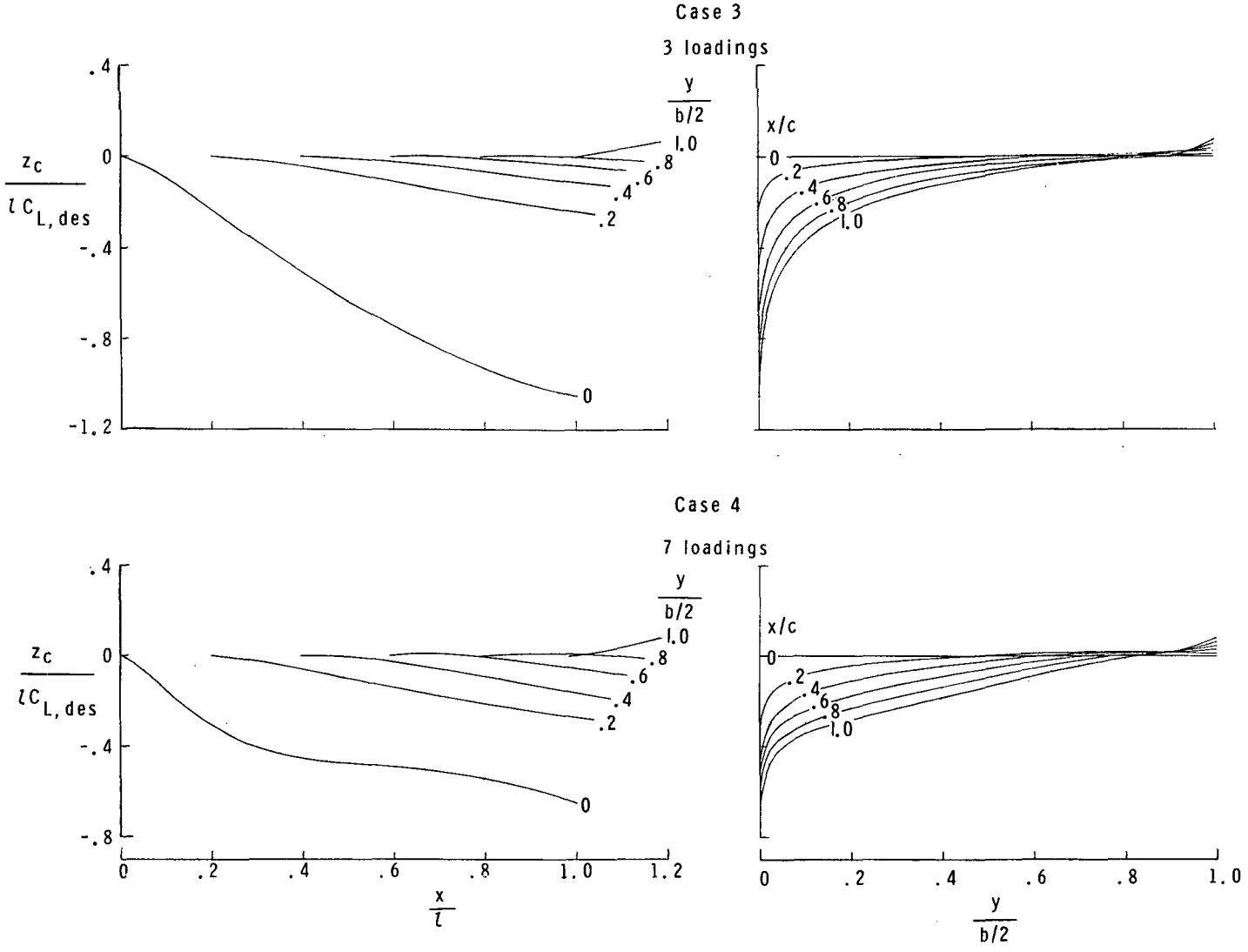

(b) Camber surfaces.

Figure 15.- Concluded.

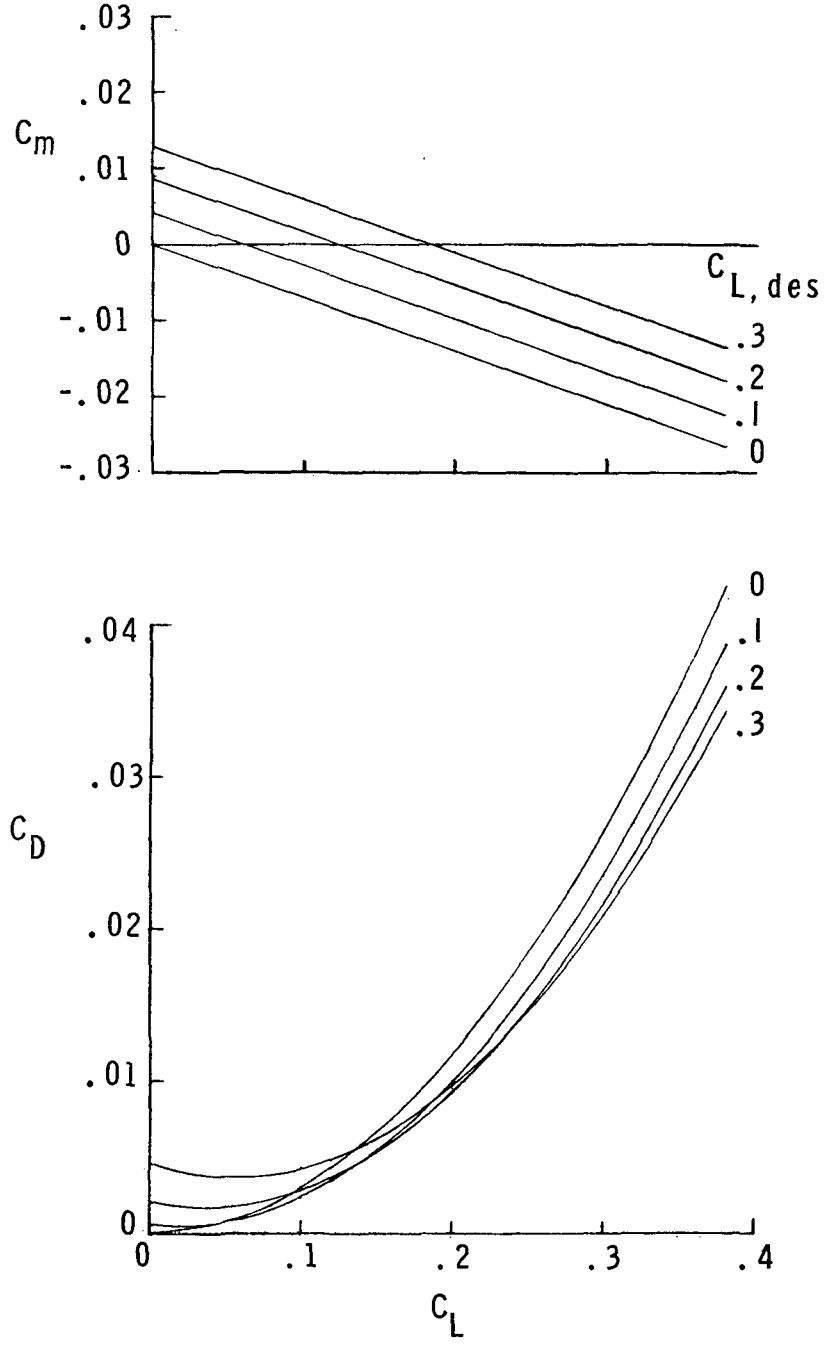

(a) Case 1, wing designed for given lift using three loadings.

Figure 16.- Theoretical drag and moment characteristics for planform B wing designs as determined by evaluation program.

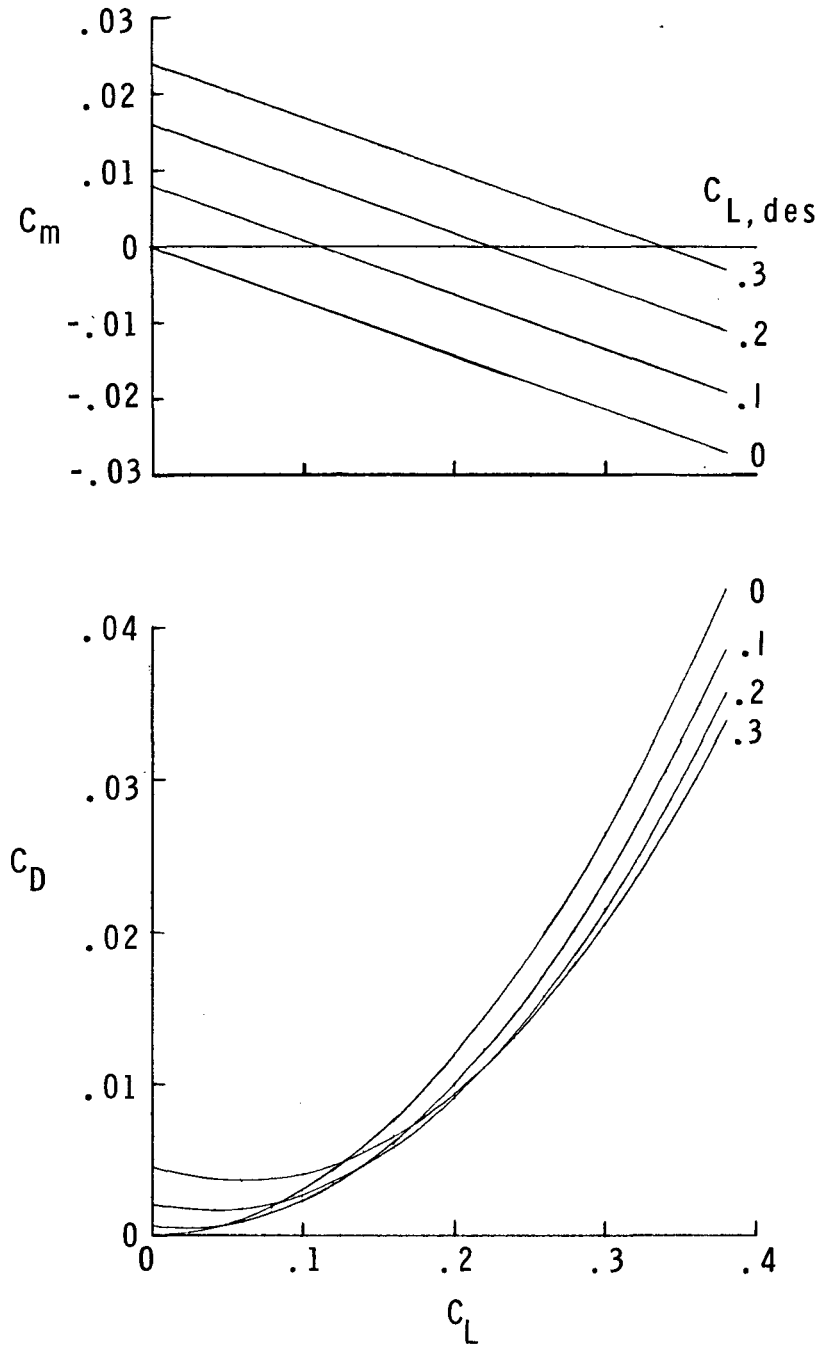

(b) Case 2, wing designed for given lift using seven loadings.

Figure 16.- Continued.

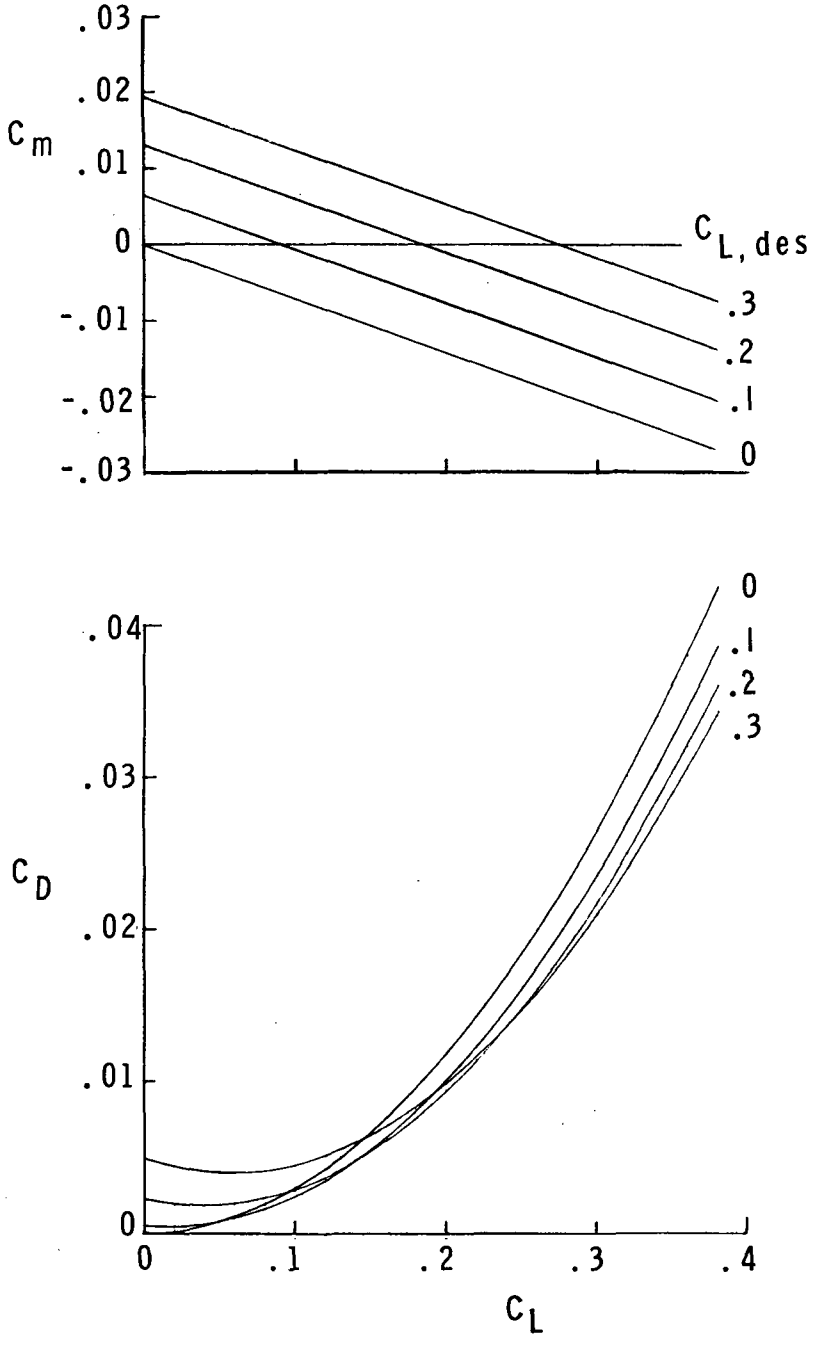

(c) Case 3, wing designed for zero moment and given lift using three loadings.

Figure 16.- Continued.

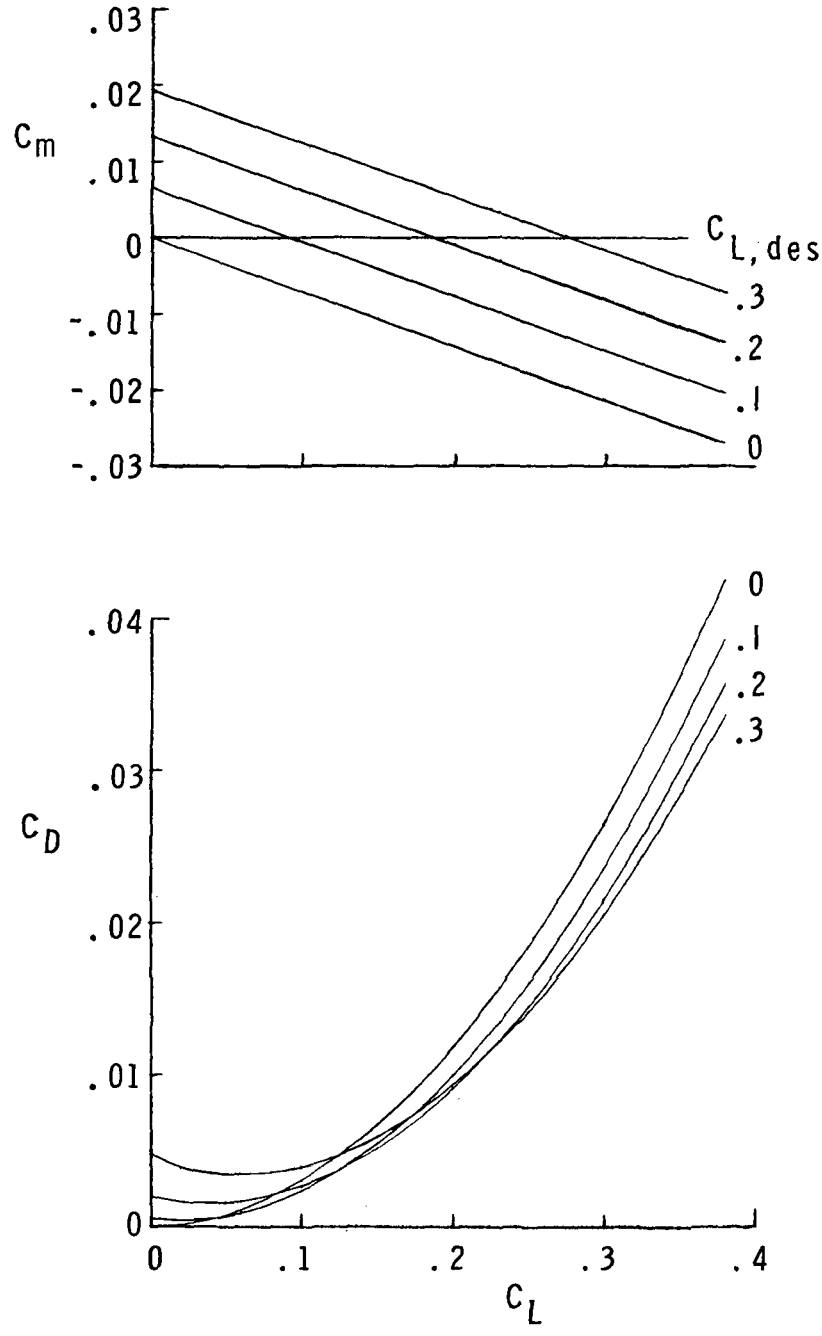

(d) Case 4, wing designed for zero moment and given lift using seven loadings.

Figure 16.- Concluded.

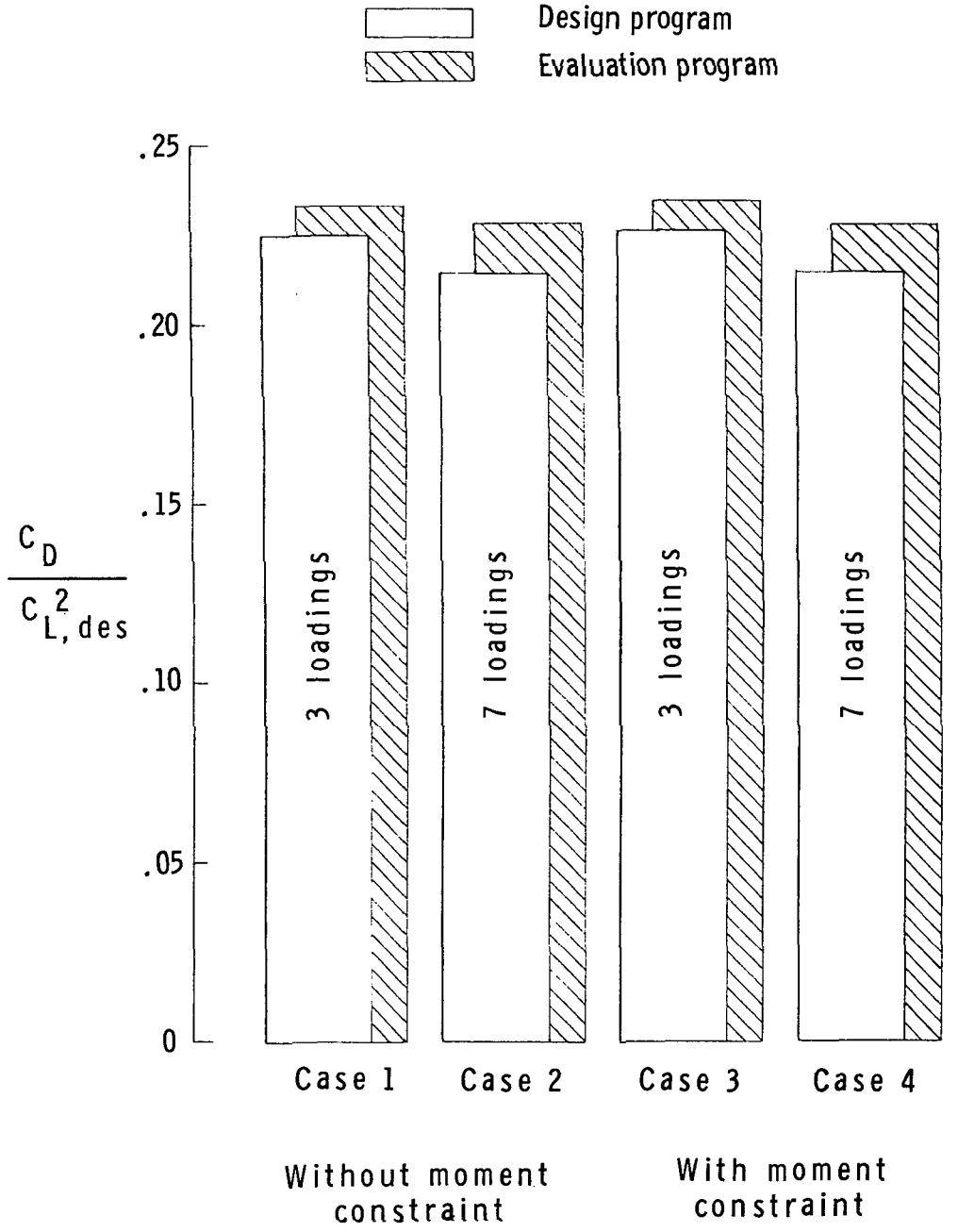

Figure 17.- Summary of effect of design program options on drag-due-to-lift factor for planform B wings.

"The aeronautical and space activities of the United States shall be conducted so as to contribute . . . to the expansion of human knowledge of phenomena in the atmosphere and space. The Administration shall provide for the widest practicable and appropriate dissemination of information concerning its activities and the results thereof."

—NATIONAL AERONAUTICS AND SPACE ACT OF 1958

NASA SCIENTIFIC AND TECHNICAL PUBLICATIONS

TECHNICAL REPORTS: Scientific and technical information considered important, complete, and a lasting contribution to existing knowledge.

TECHNICAL NOTES: Information less broad in scope but nevertheless of importance as a contribution to existing knowledge.

TECHNICAL MEMORANDUMS: Information receiving limited distribution because of preliminary data, security classification, or other reasons.

CONTRACTOR REPORTS: Scientific and technical information generated under a NASA contract or grant and considered an important contribution to existing knowledge.

TECHNICAL TRANSLATIONS: Information published in a foreign language considered to merit NASA distribution in English.

SPECIAL PUBLICATIONS: Information derived from or of value to NASA activities. Publications include conference proceedings, monographs, data compilations, handbooks, sourcebooks, and special bibliographies.

TECHNOLOGY UTILIZATION PUBLICATIONS: Information on technology used by NASA that may be of particular interest in commercial and other non-aerospace applications. Publications include Tech Briefs, Technology Utilization Reports and Technology Surveys.

Details on the availability of these publications may be obtained from:

SCIENTIFIC AND TECHNICAL INFORMATION OFFICE

NATIONAL AERONAUTICS AND SPACE ADMINISTRATION

Washington, D.C. 20546